



University of
Stavanger

FACULTY OF SCIENCE AND TECHNOLOGY

BACHELOR'S THESIS

Study programme/specialisation: Petroleum Technology	Spring/ Autumn semester, 2021.. <input checked="" type="radio"/> Open/ Confidential
Author: Liva Salomonsen <i>Liva Salomonsen</i>	
Programme coordinator:	
Supervisor(s): Pål Østebø Andersen, Dagfinn Søndena Sleveland, Dag Chun Standnes	
Title of bachelor's thesis: Experimental Analysis of Oil Recovery in Core Samples	
Credits: 20	
Keywords: Experimental Analysis of Core Samples Spontaneous Imbibition Forced Imbibition	Number of pages: ..55..... + supplemental material/other: Stavanger, 15/06/2021..... date/year

Experimental Analysis of Oil Recovery in Core Samples

Bachelor's Thesis Spring 2021

By

Liva Salomonsen

University of Stavanger

Acknowledgements

I would like to thank my supervisors Pål Østebø Andersen, Dag Chun Standnes and Dagfinn Søndena Sleveland for the academic support, input and advice they provided through the work on this bachelor's thesis.

A special thanks to Dagfinn Søndena Sleveland who taught me how to use the laboratory equipment and who always was available to help in the lab when needed.

Abstract

An experimental analysis of oil recovery in core samples during spontaneous and forced imbibition have been performed. Grey Berea sandstone cores with a permeability around 120 mD have been used in the experiments. The cores were saturated 100 % with 1.0 M NaCl, before they were drained to approximately 10 %. They were then saturated with oil, either high viscous Marcol 82, or low-viscous n-Heptane. Six spontaneous imbibition experiments, and 5 forced imbibition experiments were performed. The forced imbibition experiments were performed with two different injection rates, 2 mL/h and 15 mL/h. The effects of viscosity and different injection rates on the oil recovery were studied. The results showed that the difference in viscosity did not have a big impact on the oil recovery for the spontaneous imbibition experiments. The limiting factor in the experiments turned out to be the low relative permeability of the brine, which resisted the effect of the viscosity ratio. In the forced imbibition experiments an unexpected trend was observed where both the water permeability and the residual oil saturation decreased by each experiment performed.

List of Figures

Figure 2-1: Typical relative permeability curves during two-phase flow. S_{wc} is the saturation of the wetting fluid, and S_{nc} is the saturation of the non-wetting fluid. k_c is the relative permeability of the non-wetting fluid, while k_w is the relative permeability of the wetting fluid. Taken from (Zolotukhin & Ursin, 2000).	10
Figure 2-2: An illustration of the different wetting preferences of porous mediums. In a water-wet system, the water will cling to the rock grains, while the oil will be centered in the pores. The opposite can be seen for an oil-wet system. When the system is mixed-wet a combination of the two scenarios can be observed. (Abdallah et al., 1986).....	11
Figure 2-3: A graph of the Ma et al. dimensionless time scaling equation applied to correlate data from Mattax and KYTE (1962), Zhang et al. (1996) and Hamon and Vidal (1986). The data are gathered close to a single curve. Taken from (Ma et al., 1997).....	16
Figure 3-1: The picture to the left depicts the cores that were used in the experiments. Core 3A was used for forced imbibition with Marcol 82 as the oil, core 3B was used for forced imbibition with n-Heptane as the oil, core 3C was used for spontaneous imbibition with both n-Heptane and Marcol 82 used as the oil, and core 2C was used for spontaneous imbibition with n-Heptane as the oil. The picture to the right is of the end section of core 3A.....	19
Figure 3-2: Sketch of the experimental set-up used for spontaneous imbibition.....	24
Figure 3-3: Simplified schematic illustration of the original experimental set-up for the flooding rig. The back pressure regulator was placed before the graded burette that collected the recovered oil.	26
Figure 3-4: Simplified schematic illustration of the modified version of the flooding rig. A glass separator with a working pressure of 30 bar replaced the graded burette used earlier. The separator was placed before the back pressure regulator.	26
Figure 3-5: A detailed schematic illustration of the rig used for forced imbibition.....	27
Figure 4-1: Recovery factor plotted against time in seconds for spontaneous imbibition experiments on core samples 2C and 3C.....	33
Figure 4-2: Normalized recovery factor plotted against time in seconds for SI data on core 2C and 3C.	33
Figure 4-3: Recovery factor plotted against Ma et al. (1997) dimensionless time for spontaneous imbibition experiments on core samples 2C and 3C.	34
Figure 4-4: Normalized recovery factor plotted against Ma et al. (1997) dimensionless time for spontaneous imbibition experiments on core samples 2C and 3C.	34
Figure 4-5: Recovery factor plotted against Zhou et al. (2002) dimensionless time for spontaneous imbibition experiments performed on core 2C and 3C.	35
Figure 4-6: Normalized recovery factor plotted against Zhou et al. (2002) dimensionless time for spontaneous imbibition experiments performed on core 2C and 3C.....	35
Figure 4-7: A graph with all the oil recoveries from the different forced imbibition experiments gathered.....	42
Figure 4-8: Forced imbibition on 3A with Marcol 82 using rate 2 mL/h. Pore volumes brine injected is plotted against recovery factor and differential pressure. Disturbances can be seen on the differential pressure data. The graph has been zoomed in to the first pore volume injected to show more details.	44
Figure 4-9: Forced imbibition on 3A with Marcol 82 using rate 15 mL/h. Pore volumes brine injected is plotted against recovery factor and differential pressure. The graph has been zoomed in to the first pore volume injected to show more details.....	45
Figure 4-10: Forced imbibition repeated on 3A with Marcol 82 using rate 2 mL/h. Pore volumes brine injected is plotted against recovery factor and differential pressure. The graph has been zoomed in to the first pore volume injected to show more details.....	46

Figure 4-11: Forced imbibition on 3B with n-Heptane using rate 2 mL/h. Pore volumes brine injected is plotted against water saturation and differential pressure.....	48
Figure 4-12: Typical water-oil relative permeability curves. Taken from (Mahmood & Honarpour, 1988)	49
Figure 4-13: Comparison of repeated forced imbibition experiment on core 3A with Marcol 82 using rate 2 mL/h. Pore volumes brine injected is plotted against water saturation and differential pressure.....	50
Figure 4-14: Comparison of differential pressure recorded for all five forced imbibition experiments for the full duration of the experiments. Note that the data from experiment 3A.2nd Marcol 82 15 mL/h is plottet on the secondary vertical axix.	52

List of Tables

Table 3-1: An overview of the properties of the oils and brines used in the experiments.	20
Table 4-1: Measured properties of the cores. Only core 3C, 3A, 3B, and 3C ended up being used in reported experiments.....	30
Table 4-2: Permeability measurements for core samples 3A, 3B and 3C with gas and flooding fluids.....	31
Table 4-3: An overview of the experimental data from spontaneous imbibition experiments on cores 3C and 2C.	32
Table 4-4: Water-oil relative permeabilities and capillary pressures. Collected from (Kleppe & Morse, 1974).	36
Table 4-5: An overview of the forced imbibition data for core samples 3A and 3C.	41

Contents

ACKNOWLEDGEMENTS	2
ABSTRACT	2
LIST OF FIGURES	3
LIST OF TABLES	4
1. INTRODUCTION	7
1.1 OBJECTIVES	7
2. THEORY	8
2.1 ROCK POROSITY	8
2.2 PERMEABILITY	8
2.3 WETTABILITY	11
2.4 SATURATION.....	12
2.5 PHYSICAL FORCES INFLUENCING FLUID BEHAVIOUR AND IMBIBITION	12
2.5.1 Gravity Forces.....	12
2.5.2 Capillary Forces	13
2.5.3 Viscous Forces	13
2.6 SPONTANEOUS IMBIBITION	13
2.6.1 Scaling of Spontaneous Imbibition.....	14
2.7 FORCED IMBIBITION.....	17
2.8 VISCOSITY AND MOBILITY	17
3. MATERIALS AND METHODS	19
3.1 MATERIALS.....	19
3.1.1 Core Material.....	19
3.1.2 Oils and Brines.....	19
3.1.3 Other Chemicals.....	20
3.2 METHODS	20
3.2.1 Core Preparation	20
3.2.2 Making brine	21
3.2.3 Establishing Initial Water Saturation	21
3.2.4 Saturating the Core Samples with Oil.....	22
3.2.5 Procedure for Spontaneous Imbibition of Water	22
3.2.6 Procedure for Cleaning Cores Using Soxhlet Extractor	24
3.2.7 Experimental Set-Up of the Flooding Rig.....	25
3.2.8 Cleaning flooding rig and mounting core in core holder	27
3.2.9 Mounting core in core holder.....	28
3.2.10 Permeability Measurements	28
3.2.11 Forced Imbibition Procedure.....	29
4. RESULTS AND DISCUSSION	30
4.1 POROSITY AND PERMEABILITY MEASUREMENTS	30
4.2 PERMEABILITY MEASUREMENTS	31
4.3 SPONTANEOUS IMBIBITION RESULTS	32
4.3.1 Effect of viscosity and mobility ratio.....	35
4.3.2 Application of Scaling Models	37
4.3.3 Repeatability of the SI Experiments	38
4.3.4 Possible causes to observed differences.....	38
4.4 FORCED IMBIBITION RESULTS	41
4.4.1 Time correction of production data and delta pressure data.....	42
4.4.2 FI Experiments with Marcol 82	43
4.4.3 FI Experiments With n-Heptane.....	47
4.4.4 Trends and differences between forced imbibition experiments	48
5. CONCLUSION	52
6. SUGGESTIONS FOR FURTHER WORK	53

1. Introduction

One of the main methods to recover oil from the subsurface is by imbibition. Imbibition refers to an increase in the saturation of the wetting fluid. This can happen spontaneously or by force such as in waterfloods. (Abdallah et al., 1986) Imbibition can take place by means of gravity, capillary and viscous forces, which under different circumstances play dominant roles. During forced imbibition viscous forces dominate, while capillary forces dominate during spontaneous imbibition.

The first forced imbibition/waterflood in a reservoir happened by accident over a hundred years ago. Since then, it has gradually become one of the most widely used methods for secondary oil recovery. Forced imbibition increases oil recovery by keeping up the pressure in the reservoir, and “sweeping” the oil in front of the moving water. (Terry & Rogers, 2015, pp. 406-407) Spontaneous imbibition happens when a wetting fluid is spontaneously drawn into a porous medium by the act of capillary forces. (Morrow & Mason, 2001)

Core samples are used as models to represent reservoirs in laboratory experiments and tests. The experiments performed in this bachelor’s thesis were carried out on Grey Berea sandstone core samples, using two oils with different viscosities, one with low viscosity (n-Heptane) and one with high viscosity (Marcol 82). The forced imbibition experiments were performed using two different rates, 2 mL/h and 15 mL/h.

1.1 Objectives

The objective of this bachelor’s thesis is to perform an experimental analysis of oil recovery from core samples by forced imbibition and spontaneous imbibition. The effect of oil viscosity on the imbibition rate and ultimate oil recovery will be studied, as well as the effect of different flooding rates during forced imbibition.

2. Theory

2.1 Rock Porosity

Rock porosity is the fraction of bulk volume that is not occupied by solid particles. It is dimensionless and is referred to as a fraction or percentage. Rocks can have complex structures and vary in grain and pore sizes, thus affecting the porosity. The pore spaces can be isolated/closed or interconnected. Absolute porosity and effective porosity are two different terms being used. Absolute porosity is defined as the relationship between all pore space in a rock and the total volume of the rock. It does not matter whether the pores are interconnected or closed. The effective porosity, however, is the volume of only the interconnected pores divided by the bulk volume. This is most relevant for the experiments performed in this thesis, because it can be used as a measurement on a porous medium's capacity to store fluids such as brine and oil. Porosity can be calculated by using equation 2.1: (Zolotukhin & Ursin, 2000)

$$\varphi = \frac{V_p}{V_b} = \frac{V_b - V_m}{V_b} \quad 2.1$$

Where:

φ = porosity

V_p = pore volume

V_b = bulk volume of the rock/total volume of the rock

V_m = matrix volume/volume occupied by solid material

2.2 Permeability

Permeability is a measure of a medium's capability to transport a fluid through its network of interconnected pores. The permeability is affected by the effective porosity of the medium and the size and shape of its pores. (Zolotukhin & Ursin, 2000).

In 1856 Henry Darcy, a French physicist, derived an equation to describe linear horizontal flow. It is expressed by equation 2.6.

$$q = -A \frac{k \Delta P}{\mu L} \quad 2.2$$

Where:

q = flowrate

A = cross-sectional area of the formation

k = permeability

μ = fluid viscosity

ΔP = differential pressure

L = sample length

Absolute permeability describes a fluid's ability to flow when the porous medium is completely saturated with only one fluid. This can be calculated by using Darcy's law in equation 2.6. To be able to use Darcy's law certain conditions must be fulfilled. The flow must be horizontal, the fluid must be incompressible, the porous medium must be 100 % saturated with the fluid, the flow current must be stationary, the flow current must be laminar, and there can be no chemical or physical reactions between the fluid and the porous medium. (Zolotukhin & Ursin, 2000)

Effective permeability describes a fluid's ability to flow through a porous medium while there are other immiscible fluids present. Each fluid present will oppose the other fluids' flow, leading to a lower effective permeability compared with the absolute permeability. To calculate the effective permeability of a fluid equation 2.3 can be used. (Zolotukhin & Ursin, 2000)

$$k_e = \frac{q \mu L}{\Delta P A} \quad 2.3$$

Where:

k_e = effective permeability

q = flowrate

ΔP = differential pressure

μ = viscosity

L = sample length

A = cross-sectional area of the formation

Relative permeability relates the absolute permeability of a porous medium to the effective permeability of a specific fluid and is thus dimensionless. It is expressed by equation 2.4.

$$k_{r,i} = \frac{k_{e,i}}{k} \quad 2.4$$

Where:

k_r = relative permeability of fluid i

k_e = effective permeability of fluid i

k = absolute permeability

Relative permeability is a strong function of saturation. Typical curves of relative permeability when two immiscible fluids are present are represented in Figure 2-2.

(Zolotukhin & Ursin, 2000)

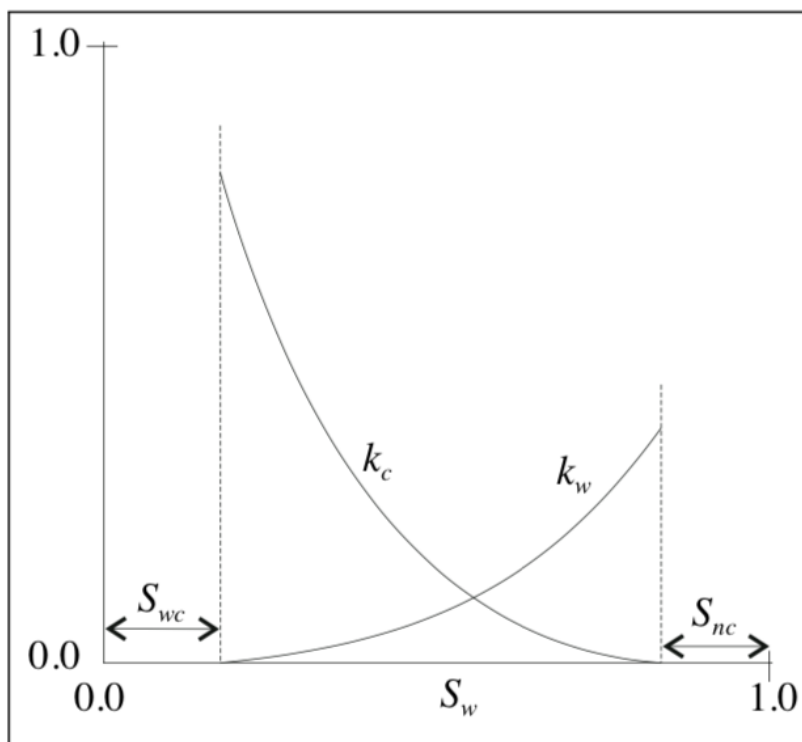


Figure 2-1: Typical relative permeability curves during two-phase flow. S_{wc} is the saturation of the wetting fluid, and S_{nc} is the saturation of the non-wetting fluid. k_c is the relative permeability of the non-wetting fluid, while k_w is the relative permeability of the wetting fluid. Taken from (Zolotukhin & Ursin, 2000).

Relative permeability data are important for calculations of multiphase fluid flow in hydrocarbon reservoirs. It is used in simulations and in order to estimate productivity, injectivity and oil recovery from reservoirs. (Mahmood & Honarpour, 1988) (Richardson, Kerver, Hafford, & Osoba, 1952). Relative permeability vs. saturation curves can be found by

displacement experiments on core samples in laboratories. There are two main methods to obtain the data: steady-state displacements and un-steady state displacement. When using the steady-state method two immiscible fluids are injected into a core sample simultaneously. The advantage with using this method is that the data is easy to interpret, but it is more time-consuming and demanding to do than the unsteady-state method. During the unsteady-state method a fluid is used to displace another immiscible fluid. With this method it is more difficult to interpret the data (Civan & Donaldson, 1989).

2.3 Wettability

Wettability can be defined as the ability a liquid has to adhere or spread to the surface of a solid material when there are other immiscible liquids present (Craig, 1971) The fluid which spreads more to a rocks surface is called the wetting phase. This fluid will cling to the matrix/grains of the rock, while the non-wetting phase will be placed more in the centre of the pores. A rock can be water-wet, oil-wet or have mixed wettability depending on the rocks wetting preference. In a water-wet rock, water will be the wetting phase, while in an oil-wet rock the oil will be the wetting phase. A rock that has neutral or mixed wettability will have an equal preference to oil and water, where the larger pore spaces are more probable to be oil-wetting while the smaller pore spaces and interstices within pores are more probable to be water-wetting. (Abdallah et al., 1986). See Figure 2-2 for an illustration of different wetting preferences in pores.

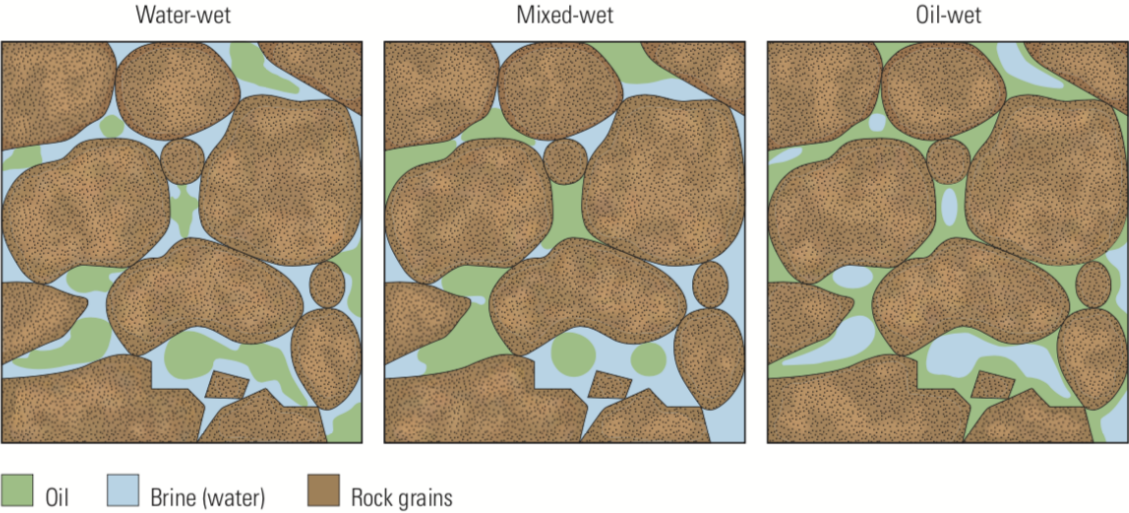


Figure 2-2: An illustration of the different wetting preferences of porous mediums. In a water-wet system, the water will cling to the rock grains, while the oil will be centered in the pores. The opposite can be seen for an oil-wet system. When the system is mixed-wet a combination of the two scenarios can be observed. (Abdallah et al., 1986)

To determine whether a rock is water-wet, oil-wet or neutral wet one can measure the contact angle. If a fluid spreads over the solid surface of a material, and thereby have a contact angle above 90 °, the surface is said to be wetting for that fluid. If the fluid instead beads up in order to minimize contact with the solid surface it will have a contact angle below 90 °, and the surface is therefore said to be non-wetting for that fluid. When the contact angle between a solid surface and a fluid is 90 °, the solid surface is said to be neutral wetting. (Zolotukhin & Ursin, 2000) (Warner, 2015, p. 31)

2.4 Saturation

In reservoir engineering, saturation is defined as the fraction of pore volume occupied by a specific fluid. Saturation is expressed by equation 2.5.

$$S_i = \frac{V_i}{V_p} \quad 2.5$$

Where:

S_i = Saturation of a fluid i, where i = water, oil, gas etc.

V_i = Volume occupied by fluid i

V_p = Pore volume

The pore volume is set to 1, and it is the sum of the volumes of different fluids present in the rock:

$$V_p = V_w + V_o + V_g = 1 \quad 2.6$$

2.5 Physical Forces Influencing Fluid Behaviour and Imbibition

There are three main forces influencing the behaviour and flow of fluids during imbibition. These are gravity forces, capillary forces and viscous forces.

2.5.1 Gravity Forces

Gravity forces are acting when there are differences in the densities of two or more immiscible fluids. When two immiscible fluids are flowing simultaneously, the fluid with the highest density will be pulled most by gravity. Water has higher density than oil and will therefore be more pulled by gravity than oil. The fluid that is less dense will flow/lay above the fluid with higher density. Gravity forces are calculated by equation 2.7. The effects of

gravity can be calculated by subtracting the water density from the oil density. (Warner, 2015, p. 40 and 102)

$$G = \rho gh \qquad 2.7$$

Where:

G = gravity force

ρ = density

g = force of gravity

h = the vertical interval of the fluid

2.5.2 Capillary Forces

Capillary forces are forces that are acting within and between immiscible fluids and the solid surface they are in contact with. Capillary action is driven by the molecular attraction between the liquids and solids. It is due to capillary forces that a fluid can flow into narrow pore channels. (Zolotukhin & Ursin, 2000)

Capillary pressure is the difference in pressure across an interface separating to immiscible fluids. It is defined as the product of the interfacial tension (IFT) and the curvature of the interface. If the curvature of the interface is concave towards the wetting fluid, a spontaneous displacement will happen if the boundary conditions let the interphase advance. (Morrow & Mason, 2001). It is the capillary pressure at the imbibition front that drives the process of imbibition (Mason & Morrow, 2013) (Leverett, 1941).

2.5.3 Viscous Forces

Viscous forces resist capillary forces. Viscous effects are related to variations and change in pressure, and are the product of the permeability, the fluid mobility and the pressure gradient. (Warner, 2015, p. 40)

2.6 Spontaneous Imbibition

Spontaneous imbibition is a process where a wetting fluid displaces a non-wetting fluid by being drawn into a porous medium by capillary forces (Morrow & Mason, 2001). The process is driven by surface energy and resisted by viscous forces. These opposing forces determine

how fast the imbibition will happen (Mason & Morrow, 2013). Oil recovery by spontaneous imbibition is important especially in fractured reservoirs with low permeabilities. The rate and amount of oil recovery are dependent on different factors involving the interactions of the crude oil/brine/rock (COBR) (Morrow & Mason, 2001). These factors include the viscosity of the wetting and non-wetting phases, fluid-fluid interfacial tension (IFT), the structure of the pores, the initial water saturation of the porous medium, and the relative permeability curves Zhou, Jia, Kamath, and Kovscek (2002). In a laboratory the imbibition rate can be measured by having a rock sample with known saturation being submerged in brine. The recovery of oil is then plotted against time. (Morrow & Mason, 2001)

2.6.1 Scaling of Spontaneous Imbibition

In order to estimate oil recovery rates from rocks with different sizes and shapes from laboratory core samples different empirical scaling models have been proposed. (Zhou et al., 2002). Mattax and Kyte (1962) introduced a scaling group where the capillary force is related to the viscous resistance. This scaling group is expressed by equation 2.6.

$$t_{DMK} = \frac{t \sqrt{\frac{k}{\varphi}} \sigma}{\mu L^2} \quad 2.8$$

Where:

t_{DMK} = dimensionless time defined by Mattax and Kyte

t = time

k = absolute permeability

φ = porosity

σ = interfacial tension

μ = water viscosity

L = a characteristic length

Six different requirements must be fulfilled in order to use this equation: (1) gravity effects must be neglected, (2) there must be identical sample shapes and boundary conditions, (3) the oil/water viscosity ratio must be duplicated, (4) the initial fluid distributions must be duplicated, (5) the relative permeability functions must be the same, and (6) the capillary pressure functions must be directly proportional. (Morrow & Mason, 2001)

Since the publication of the scaling group defined by Mattax and KYTE there has been improvements and modifications made in order to reduce the requirements listed above. New models involve a shape factor that takes size, shape and boundary conditions of the matrix into consideration. The shape factor was derived using experimental data from Aronofsky et al. (1958) and Mattax and KYTE (1962). In 1996 Zhang et al. modified the shape factor to be more accurate for sample shape and boundary conditions (Zhou et al., 2002). This shape factor has further been included in the expression for the characteristic length, L_c , which is a function of bulk volume and the area open to imbibition. It is used in order to correlate the effects of differences in sample size, shape and boundary conditions (Ma, Morrow, & Zhang, 1997). It is expressed by equation 2.9.

$$L_c = \sqrt{\frac{V_b}{\sum_{i=1}^n A_i/l_{A_i}}} \quad 2.9$$

Where:

L_c = characteristic length

V_b = bulk volume

A_i = area open to imbibition with respect to the i th direction

l_{A_i} = the distance the imbibition front travels from the imbibition face to the no-flow boundary

When studying the effect of oil viscosity on the rate of spontaneous imbibition Ma et al. (1997) found that the rate of oil recovery is proportional to the geometric mean of water and oil viscosities. The Mattax and KYTE scaling equation was modified to include the new generalized characteristic length and the geometric mean of oil and water viscosities. It is expressed in equation 2.10. The imbibition data for strongly water wet media can be correlated by plotting the percentage of oil recovery against the logarithm of dimensionless time. This has been done by Ma et al. (1997) in Figure 2-3.

$$t_D = t \sqrt{\frac{k}{\varphi}} \frac{\sigma}{\sqrt{\mu_w \mu_{nw}}} \frac{1}{L_c^2} \quad 2.10$$

Where:

t_D = dimensionless time

t = imbibition time [s]

k = absolute permeability [m^2]

ϕ = porosity [fraction]

σ = interfacial tension [N/m]

μ_w = viscosity of the wetting phase [Pa·s]

μ_{nw} = viscosity of the non-wetting phase [Pa·s]

L_c = characteristic length (function of bulk volume and the area open to imbibition) [m^{-1}]

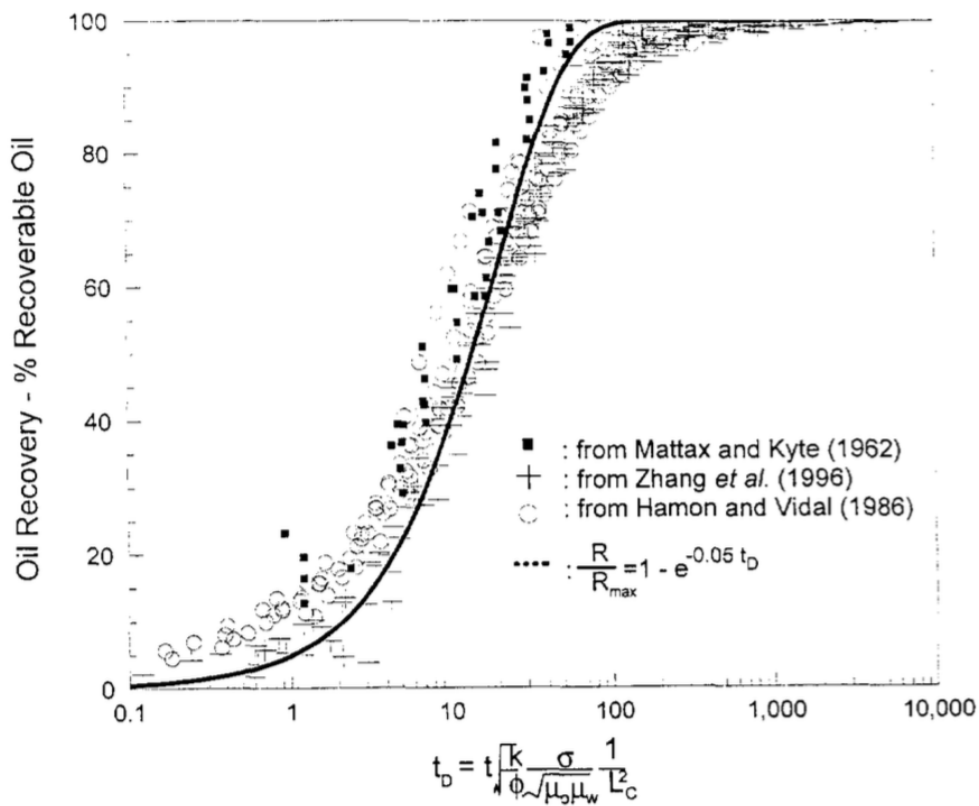


Figure 2-3: A graph of the Ma *et al.* dimensionless time scaling equation applied to correlate data from Mattax and Kyte (1962), Zhang *et al.* (1996) and Hamon and Vidal (1986). The data are gathered close to a single curve. Taken from (Ma *et al.*, 1997)

Zhou *et al.* (2002) did experiments on counter-current imbibition in low-permeability diatomite. They proposed a scaling equation that includes the characteristic mobilities and the mobility ratio of the wetting and non-wetting fluid. It is expressed in equation 2.11.

$$t_D = t \sqrt{\frac{k \sigma}{\varphi L_c^2} \sqrt{\lambda_{rw}^* \lambda_{rnw}^*}} \frac{1}{\sqrt{M^* + \frac{1}{\sqrt{M^*}}}}$$

Where:

t_D = dimensionless time

t = imbibition time [s]

k = absolute permeability [m²]

φ = porosity [fraction]

σ = interfacial tension [N/m]

L_c = characteristic length (function of bulk volume and the area open to imbibition) [m⁻¹]

λ_{rw}^* = Characteristic mobility of the wetting fluid

λ_{rnw}^* = Characteristic mobility of the non-wetting fluid

$M^* = \frac{\lambda_{rw}^*}{\lambda_{rnw}^*} =$ = Characteristic mobility ratio

2.7 Forced Imbibition

Forced imbibition or waterflooding is when oil is being displaced by forcing water through a porous medium under a pressure gradient (Morrow & Mason, 2001). It is one of the most widely used methods to improve oil recovery from a reservoir due to its effectiveness and cost-efficiency. The process of displacing oil with water is almost always an unsteady-state process. This is because the saturations of the porous medium constantly change due to the time and distance between injection and production locations. (Warner, 2015, p. 9 and 95) An ideal waterflood is piston-like, where all the oil gets produced before water-breakthrough. This is however impossible in an actual reservoir. The parameters that have the most effect on the displacement is the viscosity and mobility of the water and oil, the relative permeabilities and the formation dip. (Austad & Kolnes)

2.8 Viscosity and Mobility

Viscosity ratio and mobility ratio are two terms that are being used when describing the interaction between displacing and non-displacing fluids in two-phase flow. Viscosity describes a fluids resistance to flow. The viscosity ratio is defined as the oil viscosity divided by the water viscosity. When the viscosity of the displacing fluid is higher than that of the

fluid being displaced, the viscosity ratio is said to be favourable. If it is the other way around, the viscosity ratio is said to be unfavourable. With a favourable viscosity ratio, the displacement is stable and more effective. With an unfavourable viscosity ratio, the displacement will be unstable, and a phenomenon called viscous fingering is likely to happen. Viscous fingering means that the displacing fluid flows moves through the porous medium with finger-shaped uneven fronts, bypassing much of the oil. (Warner, 2015, p. 38) (Terry & Rogers, 2015, p. 407)

Mobility is defined as the relative permeability of a fluid divided by the viscosity of the fluid. It is expressed by equation 2.12.

$$\lambda_i = \frac{k_{r,i}}{\mu_i} \quad 2.12$$

Where:

λ_i = mobility of fluid i

$k_{r,i}$ = relative permeability of fluid i

μ_i = viscosity of fluid i

By the equation above one can say that fluids with high viscosity have lower mobility than fluids with low viscosity. One can also see that the higher the relative permeability, the higher the mobility. Mobility ratio is the relation of the mobility of the displacing/wetting phase and the mobility of the displaced/non-wetting phase. It is expressed by equation 2.13.

$$M = \frac{\lambda_w}{\lambda_{nw}} \quad 2.13$$

Where:

M = mobility ratio

λ_w = mobility of the wetting/displacing phase

λ_{nw} = mobility of the non-wetting/non-displacing phase

The mobility ratio is also described as being favourable or unfavourable. A favourable mobility ratio means that the displaced fluid has a higher mobility than the displacing/wetting fluid, and thus move with more ease in the porous medium. A high mobility ratio means that

it is unfavourable, while a low mobility ratio means that it is favourable. (Warner, 2015, pp. 38-40)

3. Materials and Methods

3.1 Materials

3.1.1 Core Material

Grey Berea sandstone was used as the core material in the experiments. It is a stone that is typically water-wetting and usually has high permeability, around 100 mD. It has been widely used in various experiments for oil recovery. Figure 3-1 shows the four cores that were used in the reported experiments.



Figure 3-1: The picture to the left depicts the cores that were used in the experiments. Core 3A was used for forced imbibition with Marcol 82 as the oil, core 3B was used for forced imbibition with n-Heptane as the oil, core 3C was used for spontaneous imbibition with both n-Heptane and Marcol 82 used as the oil, and core 2C was used for spontaneous imbibition with n-Heptane as the oil. The picture to the right is of the end section of core 3A.

3.1.2 Oils and Brines

The oils used in the experiments were n-Heptane and Marcol 82, and the brines used were 0.1 M NaCl and 1 M NaCl. 0.1 mol/L NaCl brine was used to saturate the core samples before drainage. After draining the cores to a water saturation around 10 %, the concentration of sodium chloride increased to 1 mol/L. 1 mol/L NaCl was used as the wetting fluid during

spontaneous imbibition and during flooding in the forced imbibition experiments. An overview of the properties of the oils and brines are listed in Table 3-1.

Table 3-1: An overview of the properties of the oils and brines used in the experiments.

	n-Heptane	Marcol 82	1 M NaCl	0.1 M NaCl
Viscosity¹ [cP]	0.408	31.77	1.098	0.965
Density¹ [g/mL]	0.684	0.850	1.0386	1.0024
IFT² [mN/m]	35.40	39.51	-	-

¹ Viscosity and density reported at 20 °C. All values used in calculations were corrected for actual temperature during experiment.

²IFT was measured between the oils and 1 M NaCl using a tensiometer and a platinum-ring.

3.1.3 Other Chemicals

Methanol and Toluene were used for core cleaning.

3.2 Methods

3.2.1 Core Preparation

The core material used in the experiments was Grey Berea sandstone. The cores were originally 20 cm long, and three of these were initially prepared. Each of them was divided into three parts using a Stuers Discotom 5 saw. A ruler was used to measure that the parts were approximately the same length. After each 20 cm core was divided into three parts, the cores were ground at both ends using the grinder on a GCTS Testing Systems RSG-075 2-in-1 Specimen Grinder & Saw to get perfectly perpendicular and flat end faces. The cores were named with numbers after which original core they belonged to (1-3), in addition to letters (A-C) to be able to differentiate them. One of the cores (2A) was damaged during the cutting and ended up being shorter than the others. Therefore, it was not used in the experiments. The length and diameter of each core sample was measured with a calliper and weighed. A Vinci PoroPerm instrument was used to measure the grain volume, pore volume, and gas permeability. The 1-series cores were cut before the two other sets and the pore volume and gas permeability were measured under a confining pressure of 20 bar. Later it was decided that the forced imbibition experiments were to be run under a lower net confining pressure. The pore volume and gas permeability were then measured at a confining pressure of 14 bar for core set 2 and 3.

3.2.2 Making brine

1.0 mol/L NaCl and 0.1 mol/L NaCl were used as brine for the experiments. To make the brine a 2 L volumetric flask was partially filled with distilled water. Depending on the concentration, either 116.88 g or 11.688 g of NaCl were weighed and added to the volumetric flask, along with a stirring magnet. The solution was then mixed on a magnet stirrer until the sodium chloride was completely dissolved. Distilled water was filled until it reached the 2 L mark while the magnet was temporarily held above the water. The solution was then left to stir on the magnet stirrer for approximately 15 minutes. Afterwards, the solution was filtered using a vacuum pump and a 0.65 μm filter.

3.2.3 Establishing Initial Water Saturation

For each experiment the core samples had an initial water saturation around 10%. To establish initial water saturation the core samples were saturated with 0.1 mol/L NaCl and drained to the target saturation by evaporation of water in a desiccator. The starting brine concentration was selected to give the correct brine concentration (1.0 mol/L) when the target saturation of 10% was reached.

First a clean and dry core sample was weighed, and the mass was noted. The core sample was placed in a plastic cup inside a small vacuum desiccator. A lid connected to a vacuum pump was placed over the desiccator. The vacuum pump was started, and vacuum was established inside the container. After the core sample had been under vacuum at 0.04 mbar for around 30 minutes it was saturated with 0.1 mol/L NaCl by opening a valve connected to a reservoir containing the brine. Air was not allowed to enter the vacuum chamber so as not to disrupt the vacuum. When the sample was fully submerged in brine, the valve to the reservoir and the vacuum pump was closed and the sample was allowed to rest in the chamber for approximately 30 minutes. The core sample was then taken out and rolled one turn on paper wetted with 0.1 mol/L NaCl. The two ends of the core sample were pushed one time each against the wetted paper. This was done to remove excess brine left on the outside of the core and get a consistent starting point. The core sample was weighed immediately after. It was then left in open air to evaporate for a few hours before being placed in a desiccator containing dried silica desiccant where it was drained until the water saturation reached approximately 10%. The saturation was checked repeatedly by weight until the target weight

was obtained. The initial use of evaporation in open air was done to speed up the drainage process as the evaporation in open air was several times faster than in the desiccator.

In order to predict when the core sample reached 10 % water saturation, the target weight at 10% saturation were calculated using equation 3.1.

$$m_{dry} + m_{weighing\ boat} + \frac{(m_{sat} - m_{dry} - m_{weighing\ boat})}{\rho_{0.1 \frac{mol}{L} NaCl} * \rho_{1 \frac{mol}{L} NaCl} * 0.10} \quad 3.1$$

Where:

m_{sat} = mass of the 100% water saturated core sample

m_{dry} = mass of the dry core sample

$m_{weighing\ boat}$ = mass of the weighing boat used

$\rho_{0.1 \frac{mol}{L} NaCl}$ = density of 0.1 mol/L NaCl at room temperature

$\rho_{1 \frac{mol}{L} NaCl}$ = density of 1.0 mol/L NaCl at room temperature

3.2.4 Saturating the Core Samples with Oil

After the cores had been established at an initial water saturation around 10 %, they were saturated with oil, either n-Heptane or Marcol 82. The weight and the initial water saturation were noted before the core sample was put in the vacuum desiccator. The same vacuum method was used as for saturating with water, except they were left under vacuum for shorter time to avoid evaporation of water and change in saturation. The cores were placed in the container, and the vacuum pump was turned on. They were under vacuum for about 10 minutes before the plastic cup was filled with oil. Before using the core sample for either spontaneous imbibition or forced imbibition by waterflooding it was rolled once on paper wetted with the oil. In addition, each end of the core sample was pushed lightly against the oil-wetted paper before it was weighed. This was done to remove oil on the outer surface of the cores and get a consistent saturation.

3.2.5 Procedure for Spontaneous Imbibition of Water

The spontaneous imbibition experiments were performed using an Amott cell that had been cleaned before use in a dishwasher to be as water-wet as possible. The cell was first

assembled and checked for leaks by filling it with water through a tube connected to a funnel. The two parts of the Amott cell were sealed together using grease. When the cell was leak-proof it was opened, and a coiled steel wire was put in the bottom of the Amott cell to act as a shock absorber for the core sample. A core sample with known mass, saturated with either n-Heptane or Marcol 82, was placed on top of the steel wire. A magnet was placed on the inside and outside of the top half of the Amott cell to help loosening potential oil bubbles sticking to the glass. The cell was secured using a clamp stand. A tube and funnel connected to the bottom of the Amott cell was also secured using a clamp stand. The time was started as the Amott cell was filled with 1 mol/L NaCl through the funnel and tube. The two stopcocks were closed when the meniscus reached right under 1 mL on the burette. The Amott cell was then shaken carefully in an up-and-down movement, causing oil bubbles stuck to the surface of the core sample to be released. Due to the lower density of the oil, it flowed up into the graded part of the Amott cell. The oil-gas meniscus and the oil-water meniscus were read quickly, and the time was noted. The experiment was continued by shaking the cell regularly and reading the menisci while noting the time. During tests performed earlier a camera was used to take pictures of the oil production in addition to the manual readings. From this it was observed that the manual readings matched the readings from the camera pictures well. Therefore, it was decided that manual readings would suffice. Any oil bubbles sticking to the glass was released by moving the magnet on the inside of the Amott cell with the magnet on the outside. When there was no longer any oil production the experiment was terminated. See Figure 3-2 for a sketch of the experimental set-up for spontaneous imbibition.

After the experiment the oil was removed from the Amott cell at the uppermost stopcock using a syringe and needle. This was done in a fume hood. Brine was filled at the lowest stopcock to get the oil-water meniscus up and within reach of the top of the cell. After the oil was removed, the brine was drained from the cell through the lower stopcock. The core sample was then retrieved. It was rolled once on paper wetted with the brine, and the ends was pushed against the wetted paper before it was weighed. It was then cleaned using Soxhlet.

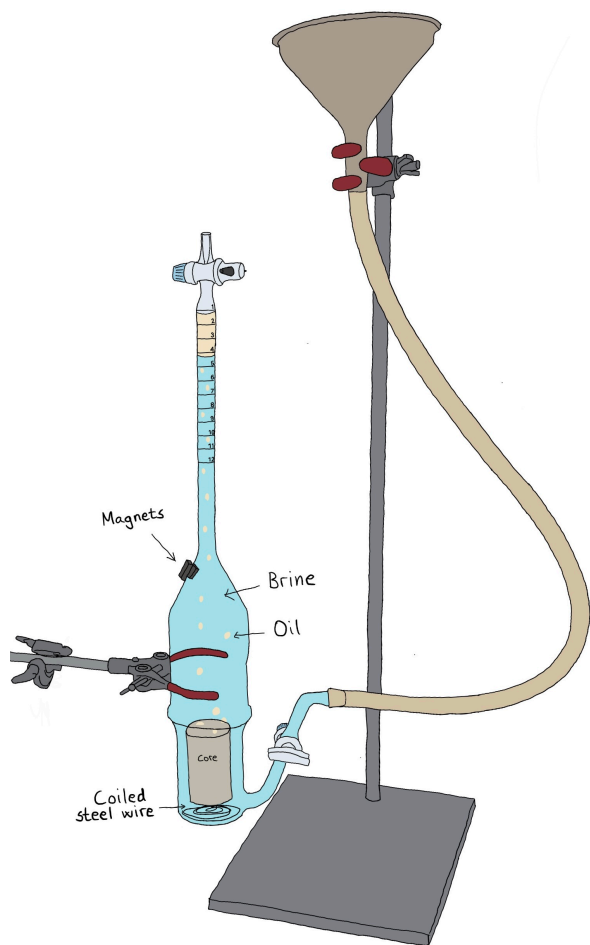


Figure 3-2: Sketch of the experimental set-up used for spontaneous imbibition.

3.2.6 Procedure for Cleaning Cores Using Soxhlet Extractor

A Soxhlet extractor was used to clean the core samples of oil, water and salts. Toluene was used to remove oils and Methanol was used to remove water and salts.

A round bottom flask containing solvent (either Toluene or Methanol) was put in a heating mantle. Boiling stones were added to the flask to avoid flash boiling and achieve more controlled boiling of the solvents. The Soxhlet extractor containing the core sample(s) was assembled on top of the round bottom flask, and over the Soxhlet apparatus an adapter and condenser were placed. All the elements were secured using stand clamps. A constant supply of cold water was supplied to the cooler and the heat was turned on. When the solvent reached the boiling point, it evaporated. The vapor traveled through the vapor arm part of the Soxhlet and reached the condenser. The hot vapor was condensed into liquid and dripped down into

the chamber where the core sample(s) was placed. The chamber was filled by the condensate and the solvents drew out the oil, salt and/or water in the core sample. When the solvent with the extract reached a certain level, it got drained out of the chamber of the Soxhlet through the siphon tube and down back into the round bottom flask. The process then started all over again, but the oil/salt/water would stay in the round bottom flask. The process would thus move oil/salt/water from the sample(s) and into the round bottom flask, thus cleaning the sample(s). When stopping the Soxhlet extractor, the heating mantle was first turned off. After the solvent and glass equipment had cooled, the cooling water was turned off.

When cleaning core samples saturated with n-Heptane, Toluene was used as solvent for one workday, and then Methanol were used for two workdays. Core samples saturated with Marcol 82 were cleaned by using Toluene and Methanol alternately for four days, starting with Toluene.

The cores were taken out of the Soxhlet extractor after three or four workdays depending on the oil they were saturated with. They were left to dry in the fume hood for a day to allow most of the methanol to evaporate, before they were placed in a heating cabinet until they were completely dried.

3.2.7 Experimental Set-Up of the Flooding Rig

The flooding rig was built from scratch in cooperation with a laboratory engineer. The rig was expanded and improved over several iterations while performing several test experiments, both permeability measurements and forced imbibition flooding.

The pump used for the flooding rig was a Quizix QX pump from Ametek Chandler Engineering. The core sample was mounted in a Hassler type core holder. The differential pressure, back pressure and overburden pressure was measured by Rosemount 3051™ Coplanar™ Pressure Transmitters. The sensor range of the two transmitters used for differential pressure measurements were 0-62 mbar for the low range, and 0-2400 mbar for the high range. The pump and datalogging was managed from a computer using the dedicated pump software PumpWorks, which is supplied by Ametek to control QX-pumps.

For the first forced imbibition experiment performed (1st flooding experiment on core 3A in Table 4-5) the rig was set up with the fluids going through the back pressure regulator before

coming out of a tubing into an upside-down graded burette filled partially by water. The oil would thus float upwards into the graded cylinder, be trapped there and the change in volume be recorded. The water produced would displace the water in the burette which would flow down into the container the burette was suspended in. See Figure 3-3 for a simplified schematic of this setup.

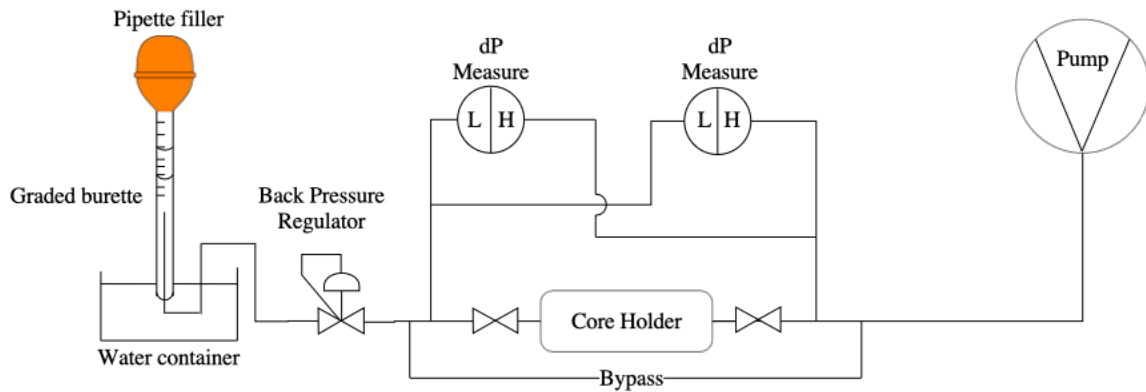


Figure 3-3: Simplified schematic illustration of the original experimental set-up for the flooding rig. The back pressure regulator was placed before the graded burette that collected the recovered oil.

Due to large disturbances in the recorded differential pressure drop data during the initial experiment the rig was altered for the remaining four experiments. It was hypothesised that small oil bubbles would build up or shift inside the back pressure regulator leading to changes in back pressure and thus changes in observed dP. A glass separator with a max working pressure of 30 bar was added to the rig, replacing the burette, to mitigate this. The separator was installed before the back pressure regulator meaning only one phase, namely water, would flow through it, thus avoiding the flooding of two phases through the regulator. This also removed the possibility of small amounts of oil getting stuck in the back pressure regulator. See Figure 3-4 for a simplified schematic of this setup.

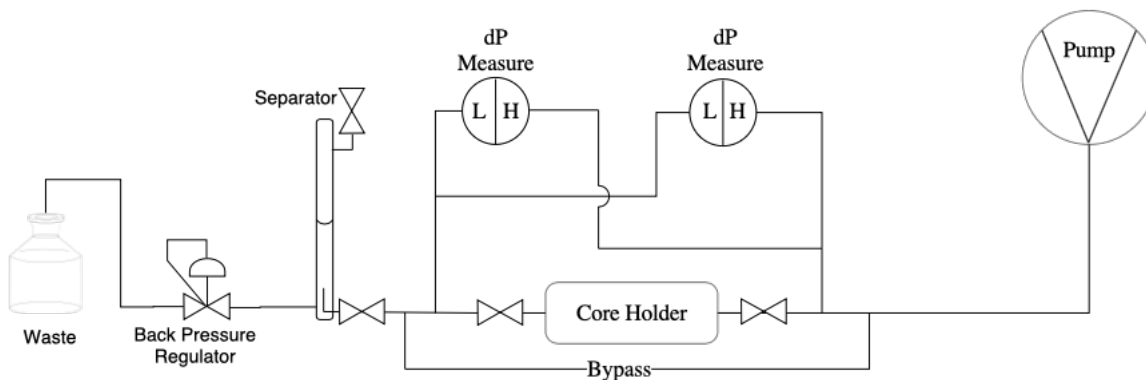


Figure 3-4: Simplified schematic illustration of the modified version of the flooding rig. A glass separator with a working pressure of 30 bar replaced the graded burette used earlier. The separator was placed before the back pressure regulator.

A Nikon D5000 DSLR camera was set on a time interval to take pictures of the oil recovery in the burette/separator. This allowed the flooding to be performed overnight and over several days without supervision and accurate volumetric readings of the meniscus. Both the burette and separator were graduated with a resolution of 0.1 mL. The meniscus could be read with an accuracy of ± 0.01 mL.

See Figure 3-5 for a detailed schematic illustration of the final version of the rig used for permeability measurements and forced imbibition experiments.

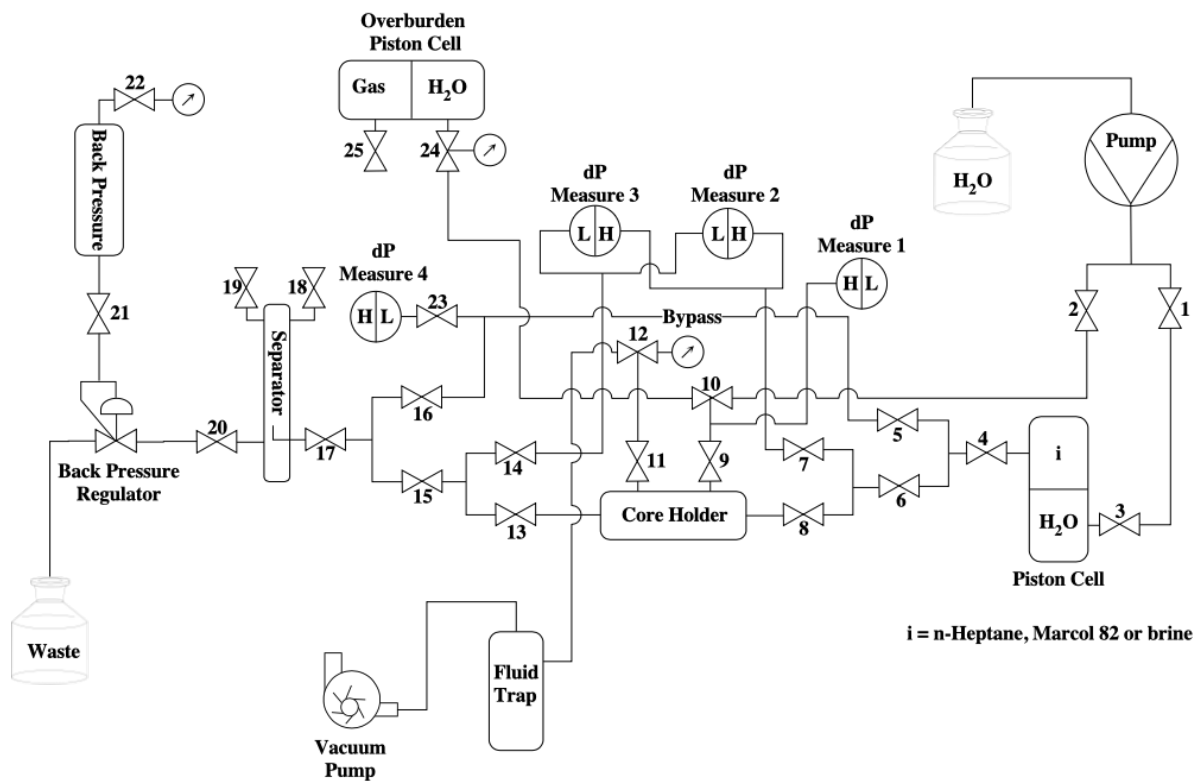


Figure 3-5: A detailed schematic illustration of the rig used for forced imbibition.

3.2.8 Cleaning flooding rig and mounting core in core holder

Before mounting a core, the tubing from valves 15 and 16 was disconnected from the separator and connected directly to the back pressure regulator. This was done to avoid filling the separator with oil during oil permeability $k_{e,o}(S_{wi})$ measurement. The valves to the pressure transducers (valve 7, 14 and 23) were closed before cleaning to avoid getting air inside the tubing leading to them. They were opened before permeability and flooding experiments. The flooding path and bypass of the system was cleaned using distilled water

(and n-heptane if Marcol 82 was used in last experiment) as well as compressed air. The empty tubing was then filled with the appropriate oil in preparation of mounting.

3.2.9 Mounting core in core holder

The core sample was mounted in a Hassler type core holder using a vacuum pump. The vacuum pump was connected to valve 12 and was used to pull the Viton sleeve in the core holder toward the walls, enabling the core to be easily pushed inside along with the end pieces. It was made sure beforehand that the valves into the cell and the valve leading to the overburden piston cell were closed (valves 8, 9 and 13). A fluid trap in front of the vacuum pump stopped the water being used as overburden fluid from entering the vacuum pump. After the core sample had been mounted in the holder, the vacuum was disconnected to allow air to enter the sleeve space and equalize the pressure. A Quizix QX pump from Ametek Chandler Engineering was used to pump water from a 2 L flask into the sleeve of the core holder (through valve 2, 10, 9, 11 and 12) removing the air now present. The core holder was rotated in a manner such that the inlet and outlet ports were facing up and all the air in the sleeve could escape and be replaced by water. Next, Valve 12 was opened towards the manometer, and valve 10 was opened towards the overburden piston cell. The core sample was put under an overburden pressure of 12 bar by slowly opening valve 24. Valve 2 were closed and valves 1, 3 and 4 were opened. The valve towards the bypass was opened (valve 5), as well as the valve at the outlet of the core holder (valve 13).

The QX pump was started, and water was pumped from the 2 L flask into a piston cell containing Marcol 82 or n-heptane depending on which oil the core was saturated with. The oil was flooded through the bypass until the backpressure reached approximately 2 bar, leaving the core sample under a net confining pressure of 10 bar. The accurate overburden and pore pressures could be read by the two pressure transducers in Figure 3-3, marked “dP Measure 1” and “dP Measure 4” respectively. The valves at the inlet of the core (valve 6 and 8) were opened and the bypass was closed. The core was then ready for measurement of effective oil permeability, $k_{e,o}(S_{wi})$.

3.2.10 Permeability Measurements

Effective oil permeability at initial water saturation, $k_{e,o}(S_{wi})$, was measured before performing the forced imbibition and spontaneous imbibition experiments. The rig was prepared by bleeding out all the tubings with the relevant oil. The core sample was placed in

the core holder and put under a confining pressure of 12 bar. Oil was flooded through the bypass in order to get the back pressure up to 2 bar. After, the valve into the core was opened and the bypass was closed. The pump was programmed to automatically measure the differential pressure drop at four different given rates over a certain time interval. Linear regression and Darcy's law was used to calculate the effective oil permeability of the core sample at an established initial water saturation at approximately 10 %.

After the forced imbibition experiments, the effective water permeability at residual oil saturation, $k_{e,w}(S_{or})$, was measured using the same method, starting with flooding brine at 4 different rates since the core and tubes already had been flooded with brine.

Relative permeability endpoints were calculated by dividing the calculated effective permeability by the gas permeability.

3.2.11 Forced Imbibition Procedure

After measurement of $k_{e,o}(S_{wi})$ the tubes of the rig carrying the flowing fluids were cleaned of oil using n-heptane and compressed air. The cleaning was performed through the bypass, leaving the inlet/outlet tubing and core between valve 8 and 13 filled with oil. Dead end tubings leading to dP's were not cleaned. The empty tubings were bled out with 1 M NaCl brine and the separator was put back in the system and air removed from tubing before tightening the connections. The core was already mounted in the core holder since $k_{e,o}(S_{wi})$ had just been measured. The core was kept at an overburden pressure of 12 bar and a pore pressure of 2 bar, giving a net confining pressure of 10 bar. Five forced imbibition experiments were performed, using two different oils (n-Heptane and Marcol 82) and two different rates (2 mL/h and 15 mL/h). The recovered oil was accumulated in the burette/separator. A camera was set to take pictures of the oil level in the burette/separator at given time intervals.

4. Results and Discussion

4.1 Porosity and Permeability Measurements

The basic measurements for each core sample are listed in Table 4-1. The length and diameter were measured using a calliper. These measurements were used to find the bulk volume, V_b , which was calculated using equation 4.1.

$$V_b = \pi * \frac{d^2}{4} * L \quad 4.1$$

Table 4-1: Measured properties of the cores. Only core 3C, 3A, 3B, and 3C ended up being used in reported experiments.

Core ID	L	D	V_b	V_m	$V_p = V_b - V_m$	V_p^1	ϕ^2	k_g^1
	[mm]	[mm]	[mL]	[mL]	atm. [mL]	10 bar [mL]	[%]	[mD]
1A	66.71	37.78	74.78	59.47	15.31	15.12	20.27	206
1B	63.66	37.78	71.36	56.69	14.67	14.42	20.28	212
1C	61.96	37.79	69.50	55.28	14.22	13.99	20.20	209
2B	66.86	37.80	75.03	59.82	15.21	14.80	19.83	148
2C	59.31	37.80	66.56	53.10	13.46	13.15	19.85	152
3A	64.94	37.82	72.95	58.64	14.31	13.93	19.19	124
3B	64.07	37.82	71.98	57.78	14.20	13.78	19.25	126
3C	65.61	37.82	73.71	59.21	14.50	14.13	19.26	128

¹ Cores 1A-1C was measured at a confining pressure of 20 bar, and cores 2B-3C were measured at a net confining pressure of 10 bar.

² Calculated based on bulk volume and grain volume at atmospheric pressure.

The matrix volume, V_m , was measured using a Vinci PoroPerm instrument. The pore volume at zero confining pressure, V_p , was calculated by subtracting the measured matrix volume from the calculated bulk volume. The pore volume and gas permeability, k_g , was also measured for each core under confining pressure. Cores 1A-1C was measured under a net confining pressure of 20 bar, while cores 2B-3C was measured under a net confining pressure of 10 bar. The porosity was calculated using equation 2.1.

The gas permeabilities were measured at atmospheric pressure, meaning they are not corrected for the Klinkenberg effect. They are therefore expected to be a little higher than the corresponding liquid permeabilities.

4.2 Permeability Measurements

The permeability measurements for cores 3A, 3B and 3C are listed in Table 4-2. Permeability was not measured for core 2C since it was only used for spontaneous imbibition and time was limited. It is assumed that the permeability is the same.

Table 4-2: Permeability measurements for core samples 3A, 3B and 3C with gas and flooding fluids.

Core ID	S_{wi} [frac]	S_{or} [frac]	Type	Perm. [mD]	Fluid
3A					
	-	-	k_g	124	Nitrogen gas
1	0.104	0.571	$k_o(S_{wi})$	102	Marcol
2	0.104	0.571	$k_w(S_{or})$	1.41	1 M NaCl
3	0.101	0.545	$k_o(S_{wi})$	87.1	Marcol
4	0.101	0.545	$k_w(S_{or})$	1.19	1 M NaCl
5	0.103	0.519	$k_o(S_{wi})$	90.5	Marcol
6	0.103	0.519	$k_w(S_{or})$	0.788	1 M NaCl
3B					
			k_g	126	Nitrogen gas
1	0.106	0.585	$k_o(S_{wi})$	81.7	n-Heptane
2	0.106	0.585	$k_w(S_{or})$	2.90	1 M NaCl
3	0.103	0.564	$k_o(S_{wi})$	83.2	n-Heptane
4	0.103	0.564	$k_w(S_{or})$	1.19	1 M NaCl
3C					
			k_g	128	Nitrogen gas
1	0.104	0.515	$k_o(S_{wi})$	111	Marcol
2	0.103	0.557	$k_o(S_{wi})$	100	n-Heptane
3	0.104	0.612	$k_o(S_{wi})$	103	Marcol

4.3 Spontaneous Imbibition Results

Spontaneous imbibition experiments were performed 4 times on core 3C, and 2 times on core 2C. n-Heptane was used as the oil for two of the experiments performed on core 3C, and Marcol 82 was used for the other two experiments. Both experiments on core 2C were done using n-Heptane as the oil. A summary of the experimental data is presented in Table 4-3.

Table 4-3: An overview of the experimental data from spontaneous imbibition experiments on cores 3C and 2C.

3C	S_{wi} [frac]	Oil	PV from weight [mL]	V_{op} [mL]	S_{or} [frac]	RF [frac]	k_o(S_{wi}) [mD]
1st	0.099	n-Heptane	13.92	4.27	0.594	0.340	-
2nd	0.104	Marcol 82	13.93	5.30	0.515	0.425	111
3rd	0.103	n-Heptane	14.12	4.80	0.557	0.379	100
4th	0.104	Marcol 82	14.07	4.00	0.612	0.317	103

2C	S_{wi} [frac]	Oil	PV from weight [mL]	V_{op} [mL]	S_{or} [frac]	RF [frac]	k_o(S_{wi}) [mD]
1st	0.100	n-Heptane	12.91	4.37	0.561	0.376	-
2nd	0.098	n-Heptane	13.02	4.47	0.559	0.381	-

All the spontaneous imbibition results have been gathered in the same graphs in order to correlate and compare them. Recovery factor has been plotted against time in seconds (Figure 4-1), and against dimensionless time, both Ma et al. (1997) and Zhou et al. (2002), (Figure 4-3 and Figure 4-5). A normalized recovery factor has also been plotted against time in seconds (Figure 4-2), and the two different equations for dimensionless time (Figure 4-4 and Figure 4-6). In the graphs where a normalized recovery has been used, all the graphs are set to finish at 1.

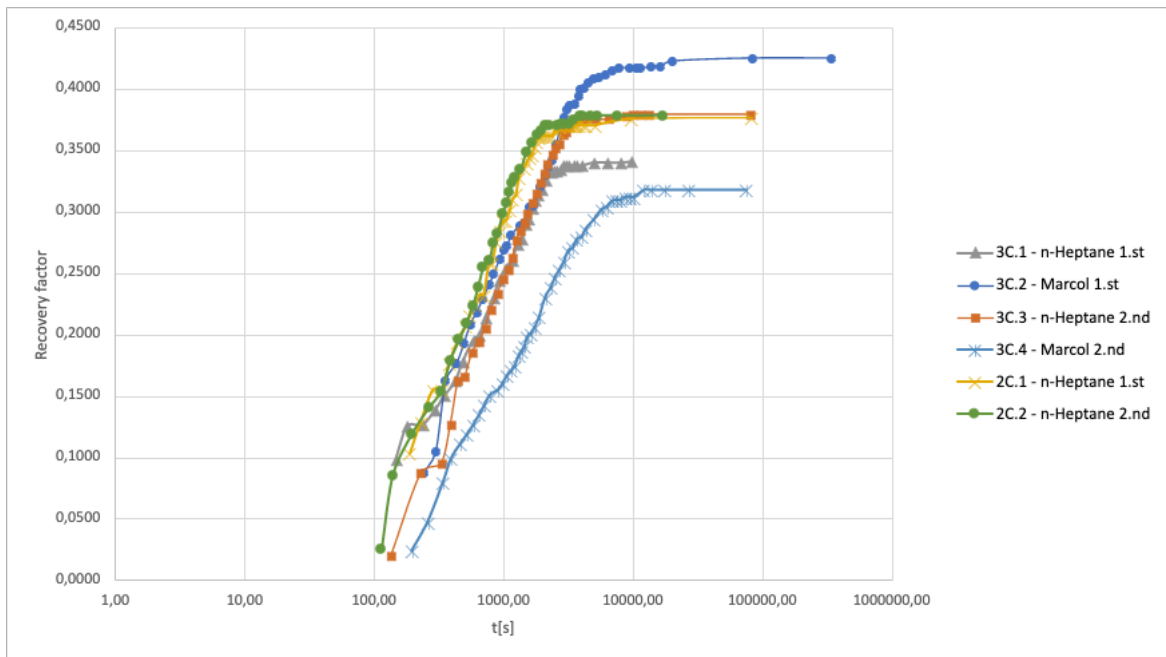


Figure 4-1: Recovery factor plotted against time in seconds for spontaneous imbibition experiments on core samples 2C and 3C.

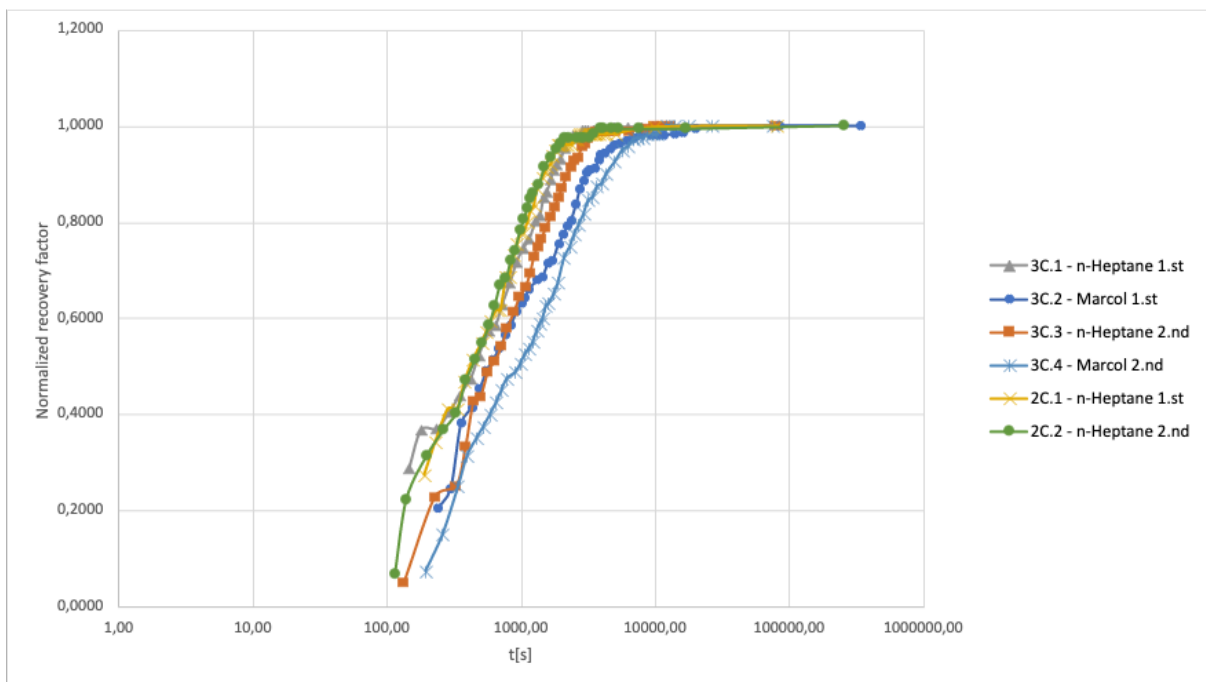


Figure 4-2: Normalized recovery factor plotted against time in seconds for SI data on core 2C and 3C.

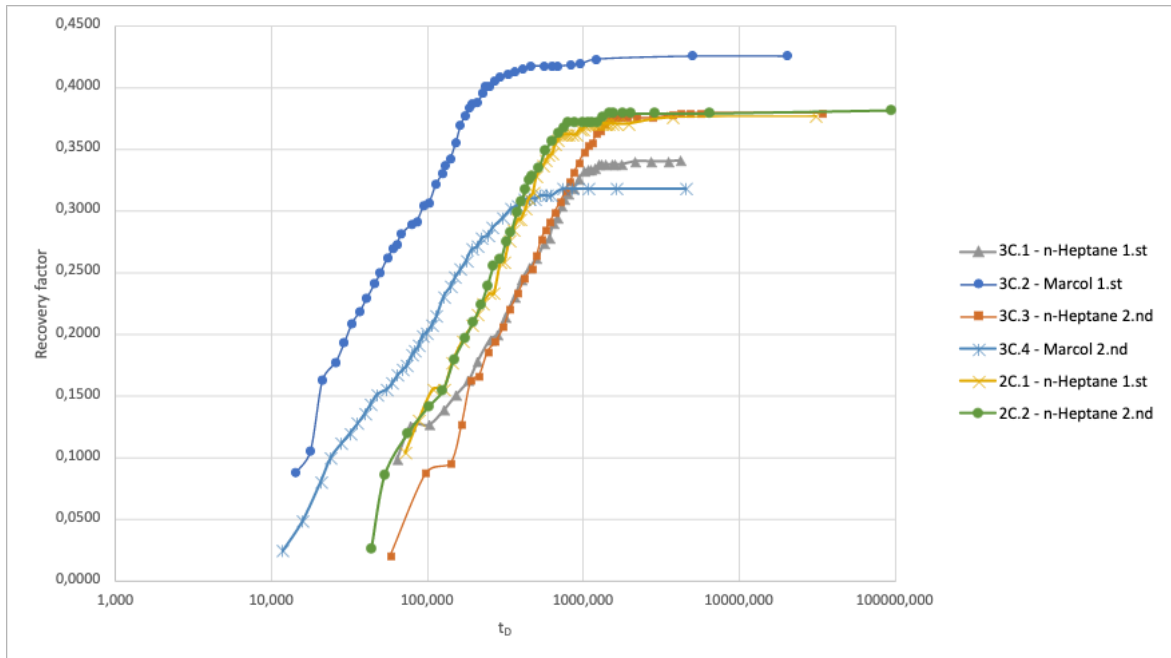


Figure 4-3: Recovery factor plotted against Ma et al. (1997) dimensionless time for spontaneous imbibition experiments on core samples 2C and 3C.

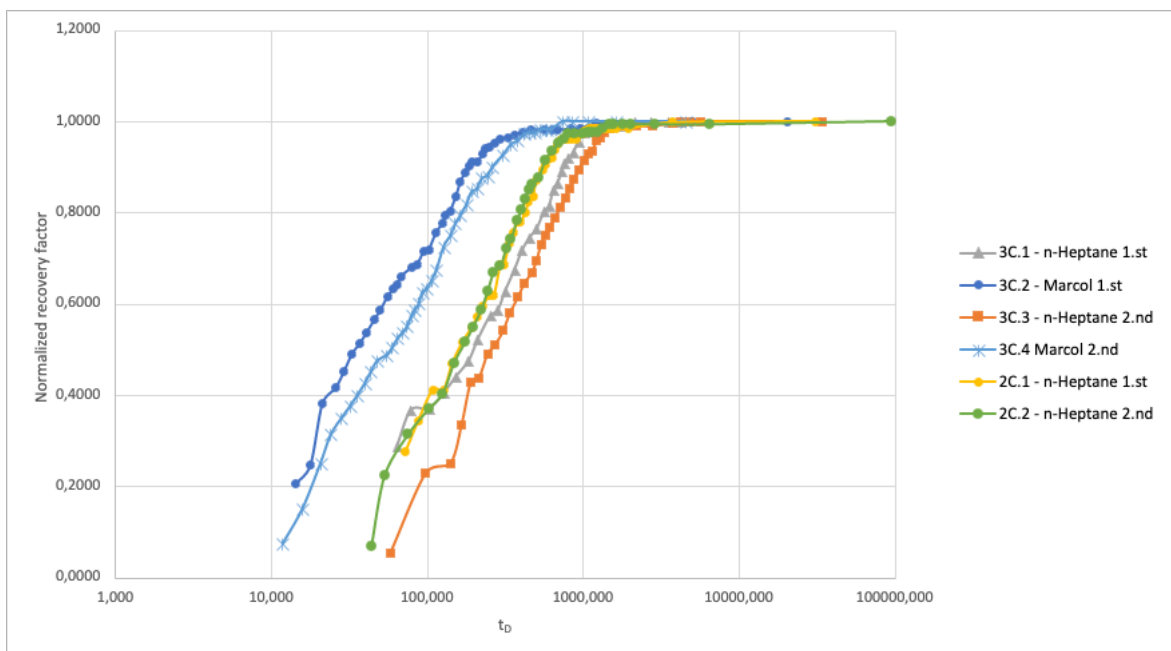


Figure 4-4: Normalized recovery factor plotted against Ma et al. (1997) dimensionless time for spontaneous imbibition experiments on core samples 2C and 3C.

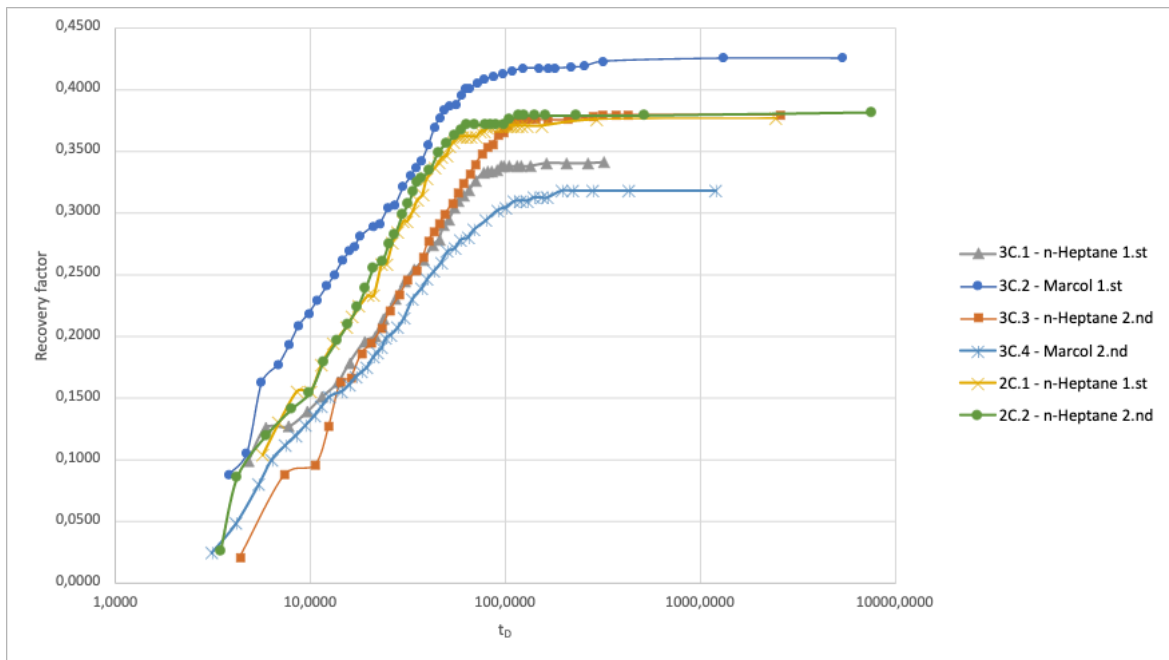


Figure 4-5: Recovery factor plotted against Zhou et al. (2002) dimensionless time for spontaneous imbibition experiments performed on core 2C and 3C.

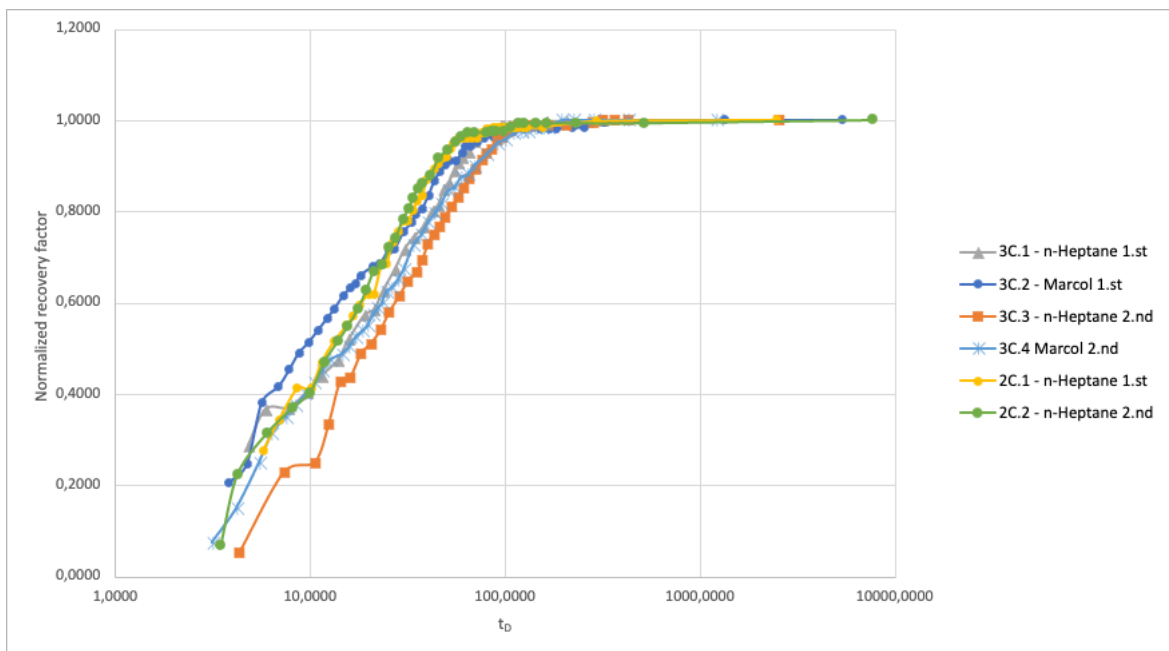


Figure 4-6: Normalized recovery factor plotted against Zhou et al. (2002) dimensionless time for spontaneous imbibition experiments performed on core 2C and 3C.

4.3.1 Effect of viscosity and mobility ratio

As one can see from the graphs, all the spontaneous imbibition experiments show a relatively linear, piston-like oil recovery, also the ones where a high viscosity oil such as Marcol 82 was used. The high viscosity of Marcol 82 (31.77 cP at 20 °C) dictates that the imbibition rate should be much slower than that of n-Heptane (0.408 cP at 20 °C), which has a much lower

viscosity. When looking at Figure 4-1 it is possible to see that one of the two experiments with Marcol 82 (experiment 3C.4) had a lower imbibition rate than those with n-Heptane, but there is not a huge difference. High viscosity oils generally have lower mobility than low viscosity oils, something that indicates that the imbibition rate and ultimate oil recovery should be lower for Marcol 82 than for n-Heptane. However, when calculating the endpoint relative permeability values, the relative water permeability is very low (0.091 for marcol and 0.016 for n-heptane). This means that the relative water permeability is resisting the effect of the viscosity of the oil. Hence, there cannot be seen a big difference in the imbibition rate for the two different oils. This indicates that the viscosity ratio does not influence the imbibition rate as much as may be expected. The limiting factor in the experiments seems to be the low relative permeability of the water/brine. The viscosity of Marcol 82 is a lot higher than the viscosity of n-Heptane, but it is not high enough to give an unfavourable mobility ratio.

Kleppe and Morse (1974) measured water-oil relative permeabilities and capillary pressure on Berea sandstone. The results they got are listed below in Table 4-4.

Table 4-4: Water-oil relative permeabilities and capillary pressures. Collected from (Kleppe & Morse, 1974).

Water-Oil Relative Permeabilities and Capillary Pressures

<u>S_o</u>	<u>k_{ro}</u>	<u>k_{rw}</u>	<u>P_c</u>
0.15	0.88	0.0000	2.75
0.20	0.75	0.0050	0.66
0.25	0.59	0.010	0.54
0.30	0.45	0.017	0.48
0.35	0.33	0.023	0.42
0.40	0.25	0.031	0.38
0.45	0.18	0.039	0.34
0.50	0.12	0.050	0.30
0.55	0.072	0.063	0.27
0.60	0.037	0.080	0.24
0.65	0.016	0.100	0.21
0.70	0.0020	0.12	0.17
0.75	0.0001	0.15	0.12
0.80	0.0000	0.19	0.05

In the spontaneous imbibition experiments performed in this bachelor's thesis, the residual oil saturation was between 0.515 and 0.612. The water permeability at S_{or} was not measured for the spontaneous imbibition experiments, so in order to calculate the endpoint relative permeabilities the data from the forced imbibition was used. The mean of the three values for $k_w(S_{or})$ with marcol was divided by the gas permeability. This gave a relative water permeability of 0.091, and a relative oil permeability of 0.75 for the experiments with Marcol 82. For the experiments with n-Heptane, the mean of the two values for $k_w(S_{or})$ on core 3B was divided by the gas permeability to find the relative endpoint permeabilities. The relative water permeability was calculated to 0.016 and the relative oil permeability was calculated to 0.65. Comparing the data from this thesis to the data from Kleppe and Morse, the relative water permeability for Marcol (0.091 vs ca. 0.080) fit quite well. The relative water permeability when using n-Heptane is too low (0.016 vs ca. 0.080) and the two relative oil permeabilities for both Marcol and n-Heptane are too high (0.75 and 0.65 vs ca. 0.037 respectively).

4.3.2 Application of Scaling Models

The Ma et al. (1997) scaling equation for imbibition rate seems to overcorrect the effect of the viscosity of Marcol 82. In the graphs where Ma et al. (1997) dimensionless time have been used (Figure 4-3 and Figure 4-4) the imbibition rate of the cores containing Marcol 82 are higher than that of the cores containing n-Heptane. This scaling equation does not include the endpoint relative permeabilities, which clearly has a great impact, and is therefore not the best choice to gather the spontaneous imbibition data. The data in the graph where no scaling equation has been used is actually more gathered than when using the Ma et al. dimensionless time.

The Zhou et al. (2002) scaling equation seems to be a better choice for scaling the spontaneous imbibition data in this bachelor's thesis. This is because this scaling equation also takes the end-point mobility ratio into consideration. In the plots where the Zhou et al. (2002) dimensionless time have been used (Figure 4-5 and Figure 4-6), the graphs of the different SI experiments gather nicely, almost to a single curve in the figure with normalized data.

4.3.3 Repeatability of the SI Experiments

The two experiments on 3C with Marcol 82 (3C.2 and 3C.4) ended up having very different results for volume oil produced and recovery factor (25% difference), as well as imbibition rate, despite it being the same core with the same initial water saturation. In the first experiment with Marcol 82 (3C.2) 5.30 mL of oil was produced, while only 4.00 mL oil was produced in the last (3C.4). The recovery factor for the experiments with Marcol 82 ended up being both higher (3C.2) and lower (3C.4) than that of the experiments with n-Heptane. The rate of imbibition of 3C.4 was substantially slower than the rest of the experiments which had quite similar rates in the linear region of the graphs.

The two SI experiments on 3C with n-Heptane (3C.1 and 3C.3) overlap very nicely in the linear region of the curves but end up on quite different recovery factors with about 10% difference between them, but far from the huge difference between the two experiments with Marcol 82. Experiment 3C.3 end up at practically the same recovery factor as the experiments with 2C.

The third experiment on 3C is more like both experiments performed on 2C regarding S_{or} and recovery factor.

The two SI experiments on 2C with n-Heptane (2C.1 and 2C.2) are almost perfectly overlapping with each other along the entire curve and show very good repeatability. They have a difference of 1% in recovery factor which is within experimental errors.

4.3.4 Possible causes to observed differences

Difference in permeability

The two experiments with n-Heptane on both 2C and 3C pair up very well in the linear region within each core. 2C.1/2C.2 imbibe at a slightly faster rate than 3C.1/3C.2. This difference in observed rate can be attributed to differences in permeability. 2C has a gas permeability of 152 mD, while 3C has 128 mD. Higher permeability gives higher imbibition rates which fits the trend shown.

It is hard to find a cause for the other variation/differences between the observed imbibition curves.

Erroneous production data

The oil being produced could be clearly seen inside the Amott cell. There was no oil stuck to the core (since it was water-wet) and there was very little getting stuck to the conical section of the Amott cell. The two magnets were used to dislodge the small amount of oil bubbles that stuck there. A couple of tests with Dean Stark to measure the remaining water in the cores after the spontaneous imbibition had finished were performed, but it had problems with water sticking to the glass ware and it was deemed that the inaccuracy in the Dean Stark analysis was larger than the inaccuracy in the measured mass balance. Since the volume of the oil can be observed directly the amount of produced oil is fully trusted.

The initial saturation is also trusted as the saturation is based on mass balance.

Cleaning

Since the cores come from a quarry that has never been exposed to hydrocarbons, they are assumed to be clean and water wet. The increase in recovery with n-Heptane from 3C.1 to 3C.3 could indicate that the cleaning between the two experiments has made the core more water wet and therefore would imbibe more water. There is no such effect observed on core 2C and the two experiments with Marcol 82 on 3C (3C.2 and 3C.4) end up at the highest and then the lowest retention factors observed of all experiments. Cleaning does not seem to explain any variation.

Wettability change

Polar components in a fluid can absorb to the rock and change the wettability to more mixed wet. n-Heptane is a pure solvent with very little contaminants of which polar components would be a tiny fraction. Marcol 82 is highly refined petroleum fraction which is catalytically hydrogenated as the final processing step to make all components fully saturated. It could still contain a small fraction of polar components which cannot be completely removed by hydrogenation. To make sure all polar components are removed, the oil could be flooded through a column of activated alumina which would absorb any polar components. This has not been performed in this thesis.

The first experiment with Marcol 82 gives higher recovery factor which is the opposite of what would be expected if the core had been made more oil wet. A wettability change is thus not believed to explain any variation.

Grain loss

When core material is used in experiments changes can occur to it which makes repeated experiments non repeatable. Grain loss from the surface of the core can occur when handling the core. A little grain loss was observed on one end face of 3C due to contact with the steel wire spiral during spontaneous imbibition experiments, but this was minor. The effect would give a systematic error and such a systematic change is not observed.

Fines migration

Flooding a core at high rates can mobilize small particles and move them around inside the core and even flood them out of the core itself. This can change the pore structure, increase/decrease permeability in some regions of the core and give a difference response between sequential experiments. Harsh cleaning protocols like Soxhlet can also damage core material, as well as saturation by vacuum due to the quickly moving liquid fronts. Well consolidated sandstone material was specifically selected for this thesis to avoid as much as possible of these potential problems, but it cannot be ruled out that the core material was damaged. Since 2C give such good repeatability, it is not expected to have occurred with this core. Permeability was also not measured on 2C while 3C was measured several times. There are large changes in recovery factor in 3C, but it would be expected that core damage would give a trend that develop in one direction, which does not fit with the large changes back and forth that are observed between the four experiments on the core. In lack of other causes fines migration is a possible cause to some of the observed differences between the experiments of core 3C.

4.4 Forced Imbibition Results

Forced imbibition experiments were performed on core samples 3A and 3B. They come from the same original 20 cm core and therefore have similar properties. Marcol 82 was used as the oil in experiments on 3A, while n-Heptane was used in experiments on 3B. Two different rates were used during the experiments, 2 mL/h and 15 mL/h. See Table 4-5 for an overview of the experimental data, and

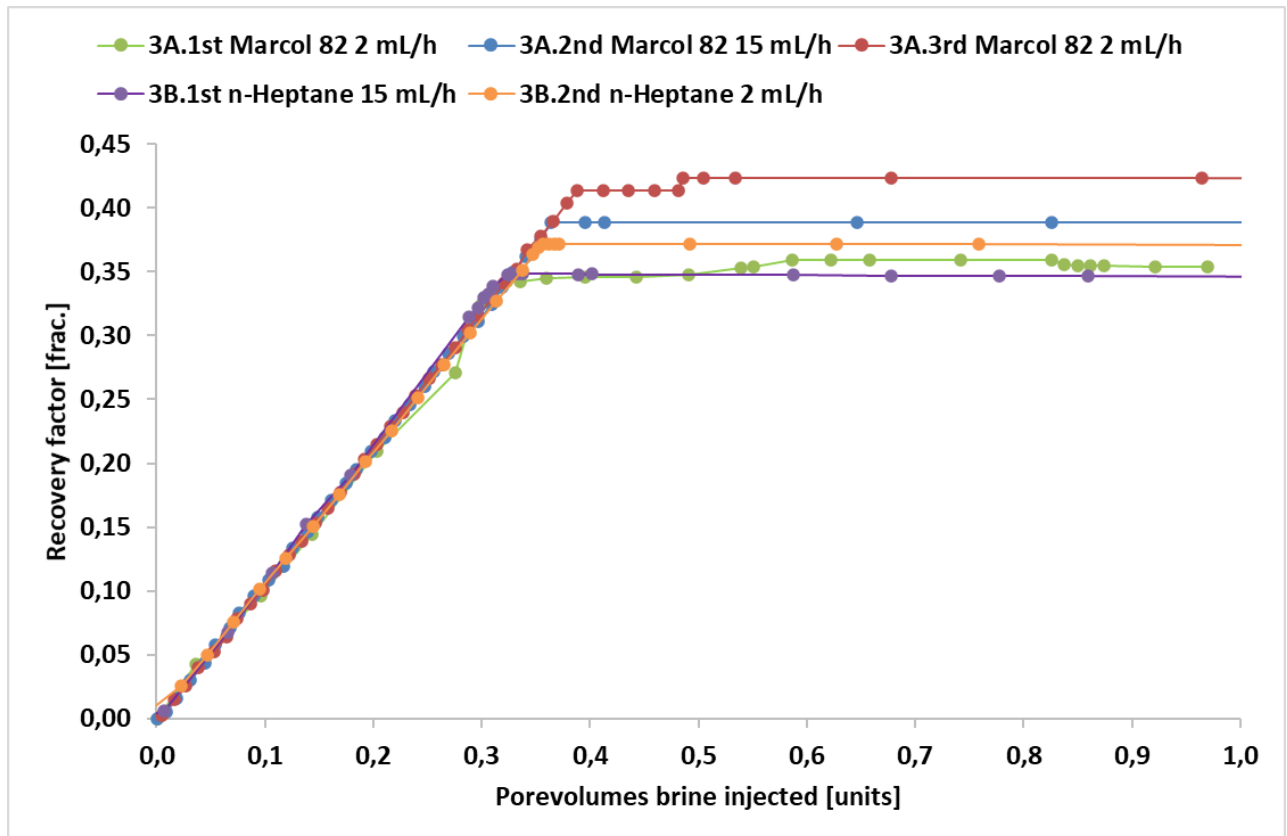


Figure 4-7 for a graph showing the recovery factor for all the experiments.

Table 4-5: An overview of the forced imbibition data for core samples 3A and 3C.

Core	Exp nr.	k_g [mD]	$k_{e,o}(S_{wi})$ [mD]	$k_{e,w}(S_{or})$ [mD]	$k_{r,o}(S_{wi})$ [mD]	$k_{r,w}(S_{or})$ [mD]	Oil used	Rate [mL/h]	S_{wi} [frac.]	S_{or} [frac.]	RF [frac.]
3A	1		102	1.41	0.82	0.01	Marcol 82	2	0.104	0.571	0.363
	2	124	87.1	1.19	0.70	0.01		15	0.101	0.545	0.394
	3		90.5	0.788	0.73	0.01		2	0.103	0.519	0.422
3B	1	126	81.7	2.90	0.65	0.02	n-Heptane	15	0.106	0.585	0.346
	2		83.2	1.19	0.66	0.01		2	0.103	0.564	0.371

The oil permeability at initial water saturation, $k_o(S_{wi})$, and the water permeability at residual oil saturation, $k_w(S_{or})$, were calculated using equation 2.3. The end-point relative

permeabilities were calculated using equation 2.4, where the gas permeability was used as the value for the absolute permeability.

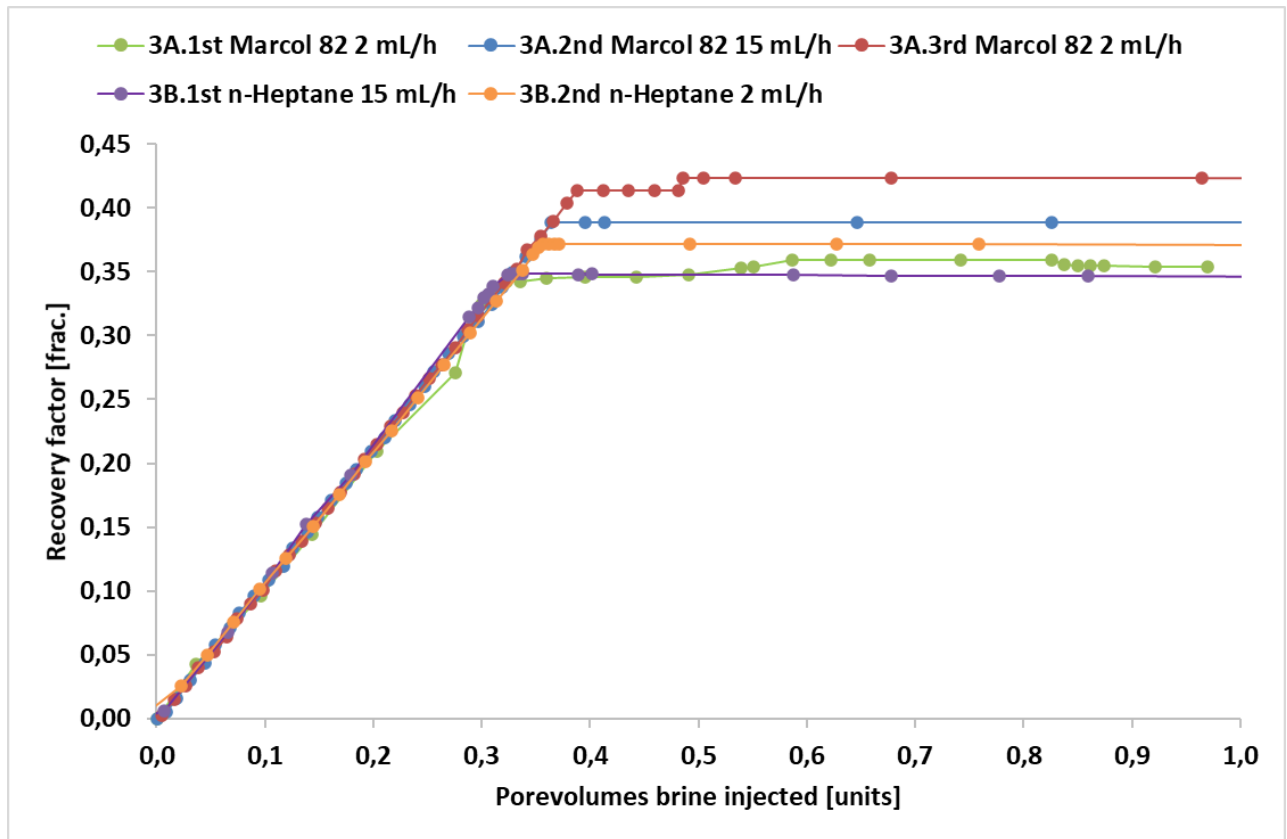


Figure 4-7: A graph with all the oil recoveries from the different forced imbibition experiments gathered.

4.4.1 Time correction of production data and delta pressure data

The dP is recorded by the computer without a time delay. When the flooding is started the inlet tubing into the core holder is filled with the oil the core is saturated with. The initial dP recorded is thus due to oil moving through the core and not brine. The dead volume in the inlet tubing was measured by filling the empty tubing with water from the pump and reading off the injected volume. Several measurements were performed, and the average was used. This volume is used to calculate a “corrected porevolumes injected” based on the pump rate being used such that the start of the graph should show the dP when water first hits the core.

In contrast to the dP, the production data cannot be recorded until the produced oil reaches the separator and can be measured there. This leads to a time delay between the two measurements. The production data can either be corrected by measuring the dead volume from the outlet of the core holder to the separator and using that to correct the time, or correct it based on the dead volume in the inlet tubing. In this thesis the last option was used as it is

more accurate measuring one tubing than several tubes going through several valves. The production curve was moved so that initial production would correspond with origin in the graph.

Since both the inlet and outlet tubings between valves 8 and 13 contain oil when the flooding is started this oil must be subtracted from the volume of produced oil. This has been done in all data presented in this thesis. The time adjustment of the production data discussed above incorporates this correction.

4.4.2 FI Experiments with Marcol 82

Three experiments were performed on 3A, all using Marcol 82 as the non-wetting phase. Two different flooding rates were used, 2 mL/h and 15 mL/h.

Recovery factor and delta pressure over the core is plotted against pore volumes brine injected for all three experiments given in Figure 4-8, Figure 4-9 and Figure 4-10.

3A.1st Marcol 82 2 mL/h

The first experiment on 3A was performed using the initial experimental set-up (see Figure 3-3) where the back pressure regulator was placed before the graded burette where the oil/water level was read. This led to disturbances in the differential pressure data, most likely because of small drops of oil getting trapped or shifting inside the back pressure regulator. . See Figure 4-8 for a graph showing the data.

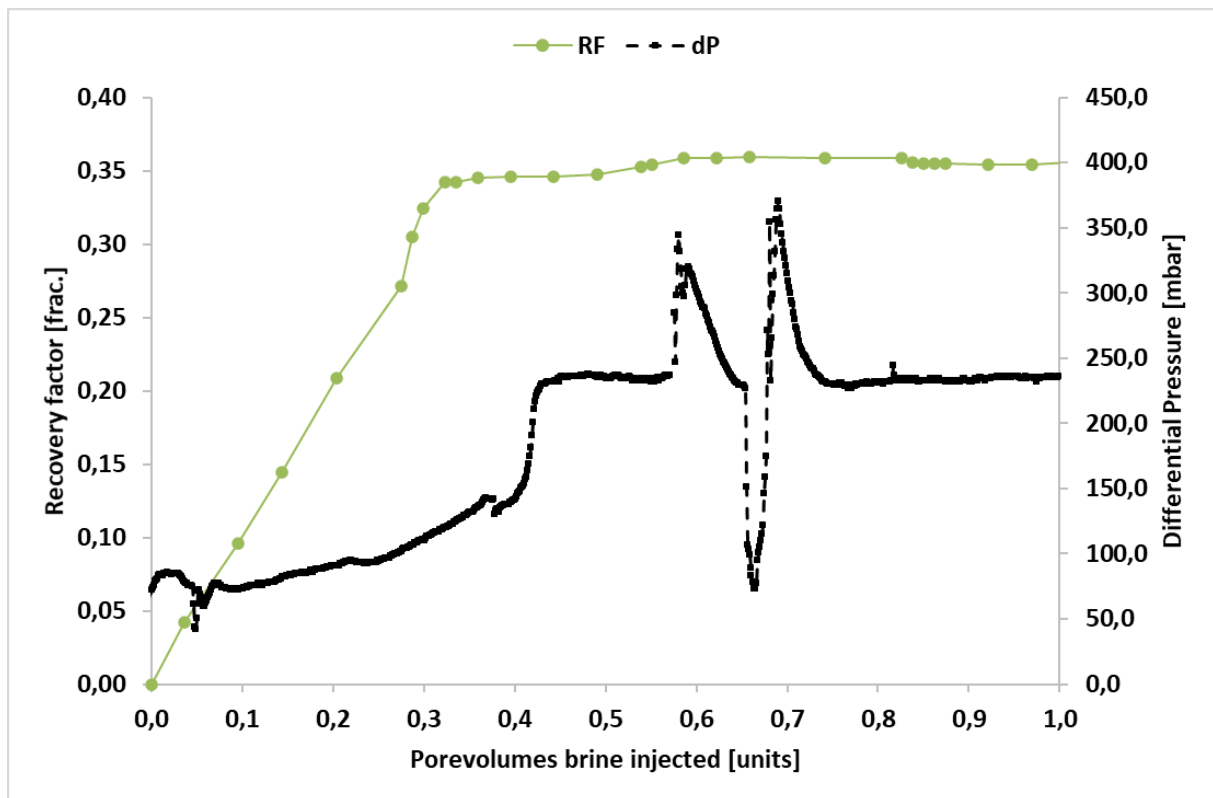


Figure 4-8: Forced imbibition on 3A with Marcol 82 using rate 2 mL/h. Pore volumes brine injected is plotted against recovery factor and differential pressure. Disturbances can be seen on the differential pressure data. The graph has been zoomed in to the first pore volume injected to show more details.

3A.2nd Marcol 82 15 mL/h

The second experiment performed on core 3A was with the modified set-up where the burette was replaced by a separator placed in front of the back pressure regulator (see Figure 3-5 and Figure 3-4). Disturbances were no longer seen on the differential pressure data and the

production data was more stable. See

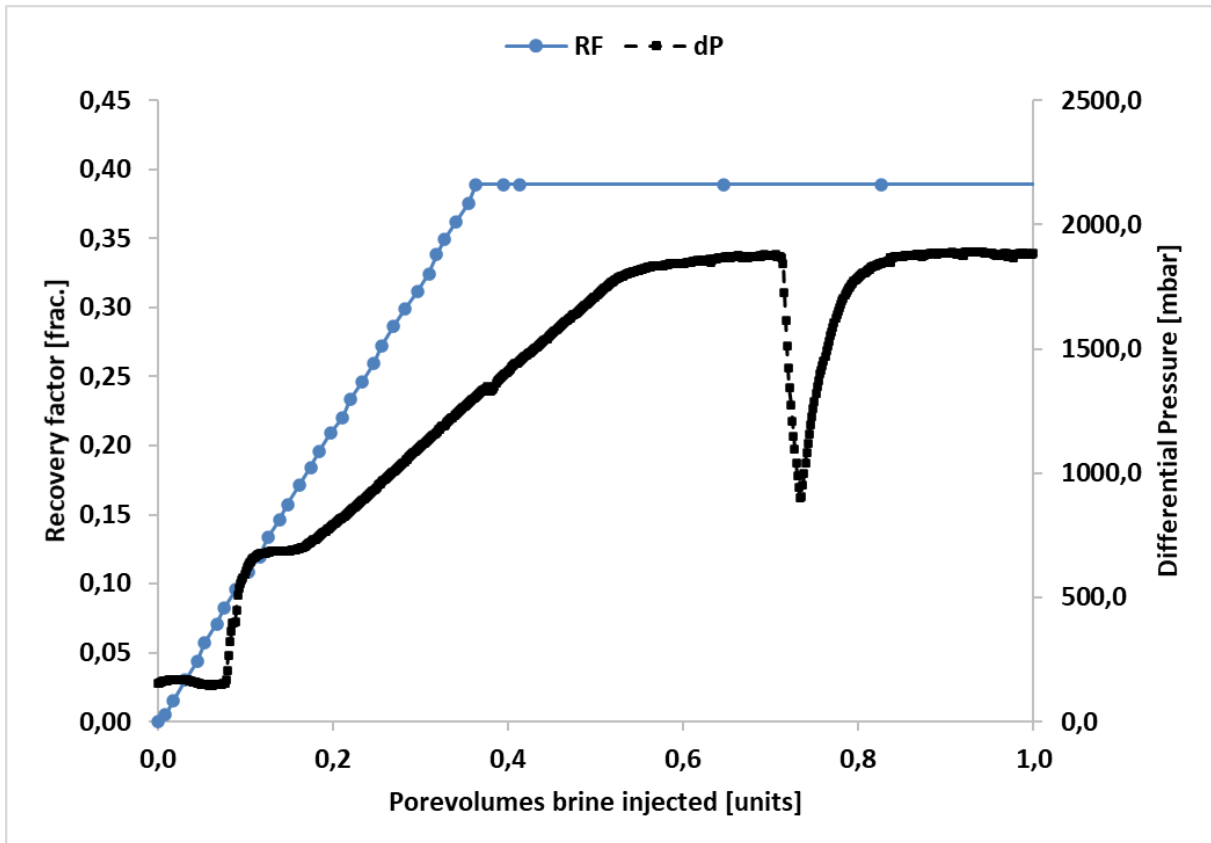


Figure 4-9 for a graph showing the data. The sudden dip in the dP that can be observed is caused by the pump being stopped momentarily due to the pump going over the set safety pressure. Due to a mistake the pore pressure had not been increased before starting the experiment. This caused the dP to initially stabilize at a low plateau (about 150 mbar), before increasing as expected when the system had been pressurized to the setback pressure.

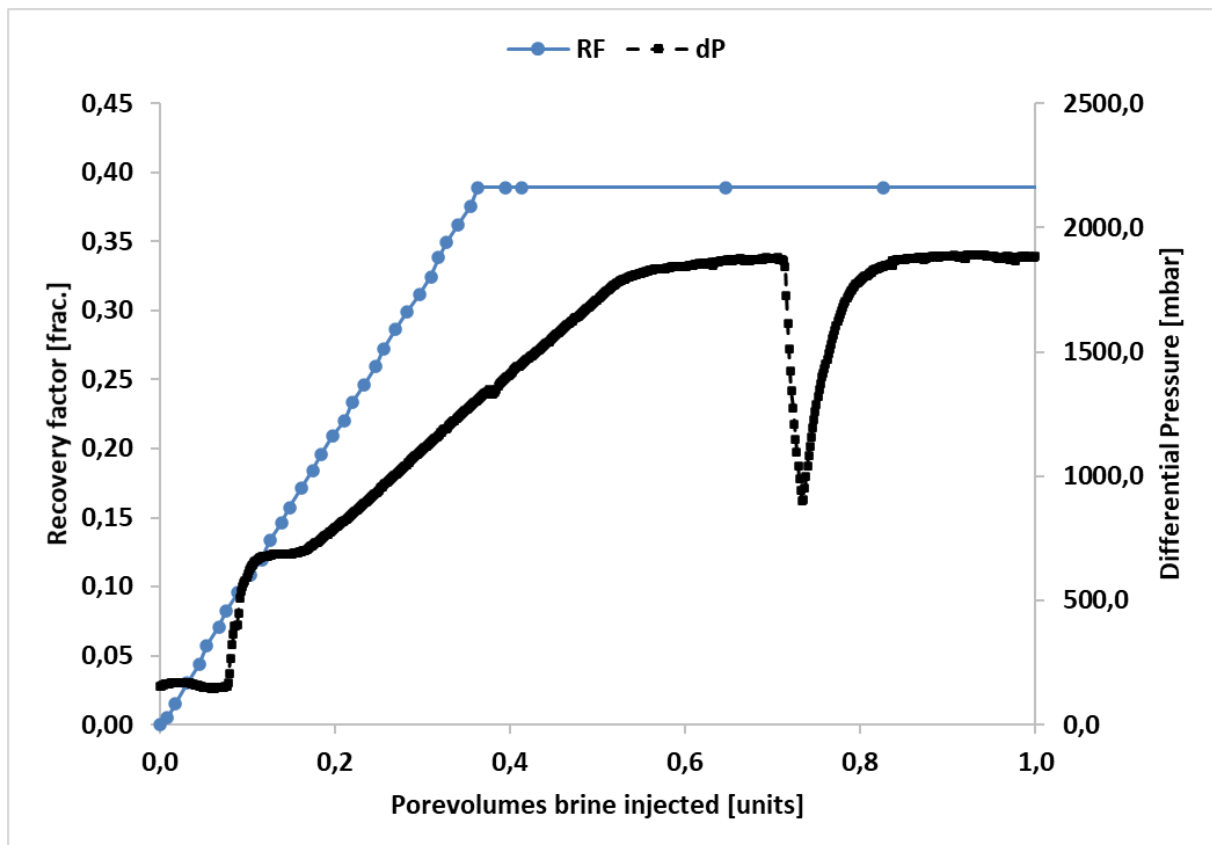


Figure 4-9: Forced imbibition on 3A with Marcol 82 using rate 15 mL/h. Pore volumes brine injected is plotted against recovery factor and differential pressure. The graph has been zoomed in to the first pore volume injected to show more details.

3A.3rd Marcol 82 2 mL/h

Due to the disturbances on the differential pressure data and possibility of trapped oil in the back pressure regulator in the first experiment performed on core 3A with Marcol 82 and pump rate 2 mL/h, the experiment was repeated with the new set-up to get data without any disturbances. It was also repeated to check the repeatability of the experiments. See Figure 4-10 for a graph showing the data.

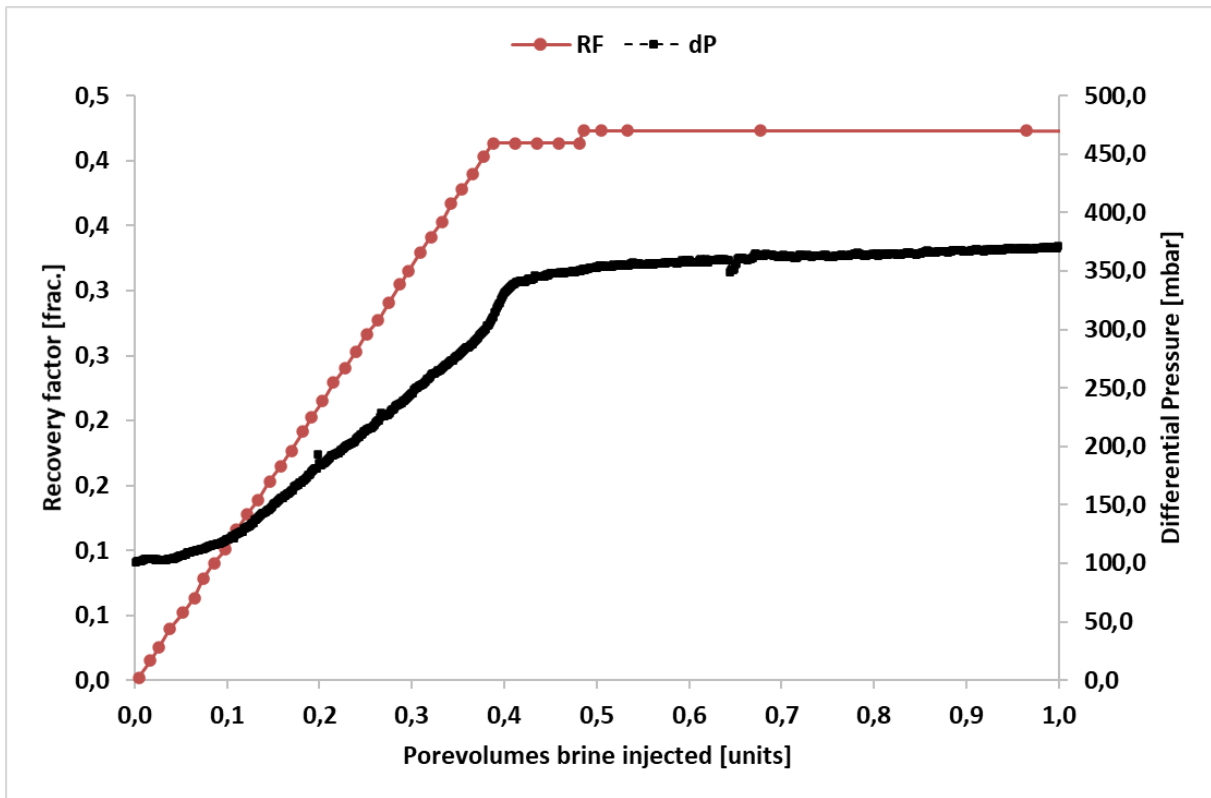


Figure 4-10: Forced imbibition repeated on 3A with Marcol 82 using rate 2 mL/h. Pore volumes brine injected is plotted against recovery factor and differential pressure. The graph has been zoomed in to the first pore volume injected to show more details.

FI Experiments With n-Heptane

Two experiments were performed on core 3B, both using n-Heptane as the non-wetting phase. Two different rates were used, 2 mL/h and 15 mL/h.

3B.1st n-Heptane 15 mL/h

A rate of 15 mL/h was used during the first experiment performed on core 3B. A graph from the experiment is presented in **Feil! Fant ikke referansebildet..**

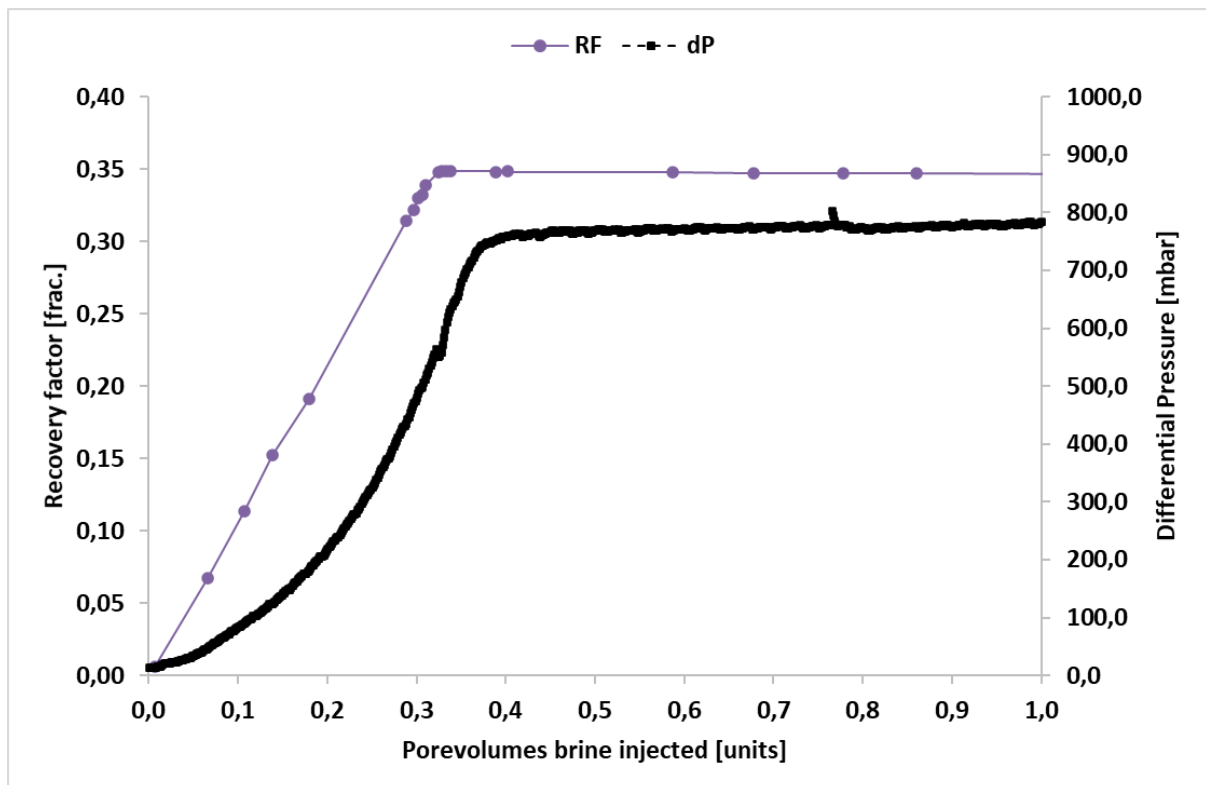


Figure 4-11: Forced imbibition on 3B with n-Heptane using rate 15 mL/h. Pore volumes brine injected is plotted against recovery factor and differential pressure. The graph has been zoomed in to the first pore volume injected to show more details.

3B.2nd n-Heptane 2 mL/h

The second experiment with n-Heptane on core 3B was performed with an injection rate of 2 mL/h. A graph from the experiment is presented in Figure 4-12.

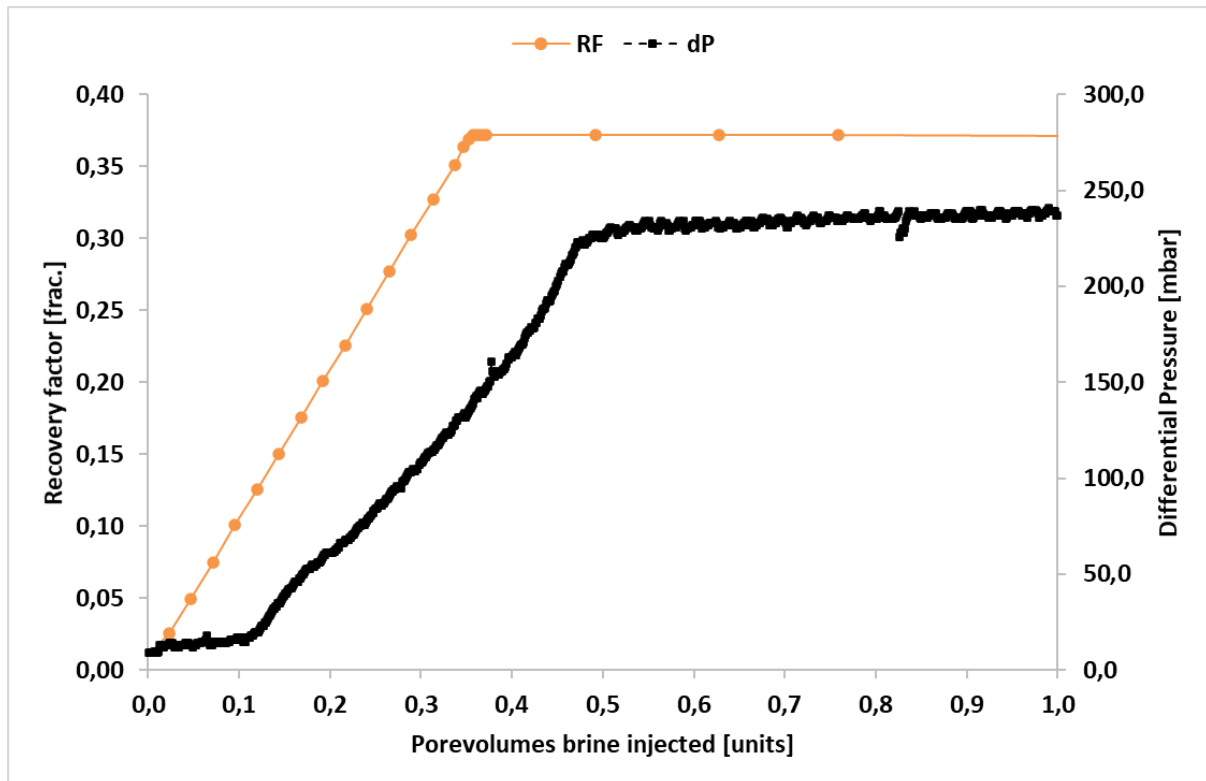


Figure 4-12: Forced imbibition on 3B with n-Heptane using rate 2 mL/h. Pore volumes brine injected is plotted against water saturation and differential pressure.

4.4.3 Trends and differences between forced imbibition experiments

Two trends can be observed from the gathered forced imbibition data. After each experiment the permeability of water at residual oil saturation, $k_w(S_{or})$, and S_{or} decreases, and the recovery factor increases. From the literature (Odeh & Dotson, 1985) it is expected that when S_{or} decreases, the relative water permeability increases, which is the opposite of what can be observed in these experiments. A typical water saturation vs. relative permeability curve for water-wet mediums is illustrated in Figure 4-13. From the figure it is clear that with a decrease in residual oil saturation, the relative permeability of water should increase. For

some reason the opposite effect can be seen in the results of this thesis. This could possibly be due to physical changes in the cores. The cores have been used for forced imbibition more than once, and several changes could have happened to the cores between each experiment as discussed in section 4.3.4. For example due to harsh cleaning with Soxhlet, the flooding, handling of cores etc.

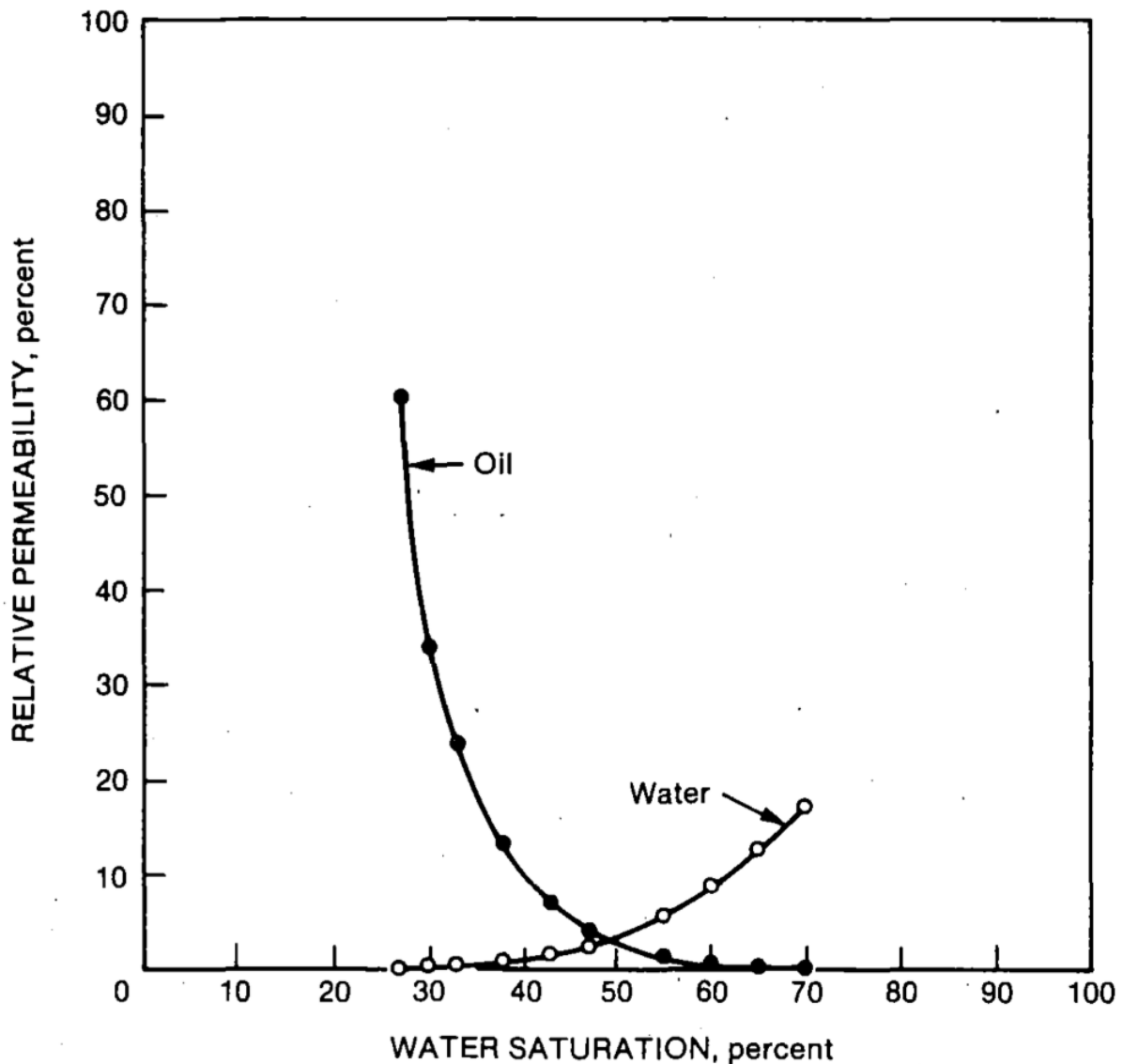


Figure 4-13: Typical water-oil relative permeability curves. Taken from (Mahmood & Honarpour, 1988)

The experiment with Marcol 82 at 2 mL/h on core 3A was repeated using the separator instead of the burette. As shown in Figure 4-14 the second experiment gave a substantially higher delta pressure and recovery factor than the initial experiment. As seen with the other

experiments a higher water saturation gives a higher delta pressure and thus a lower relative water permeability.

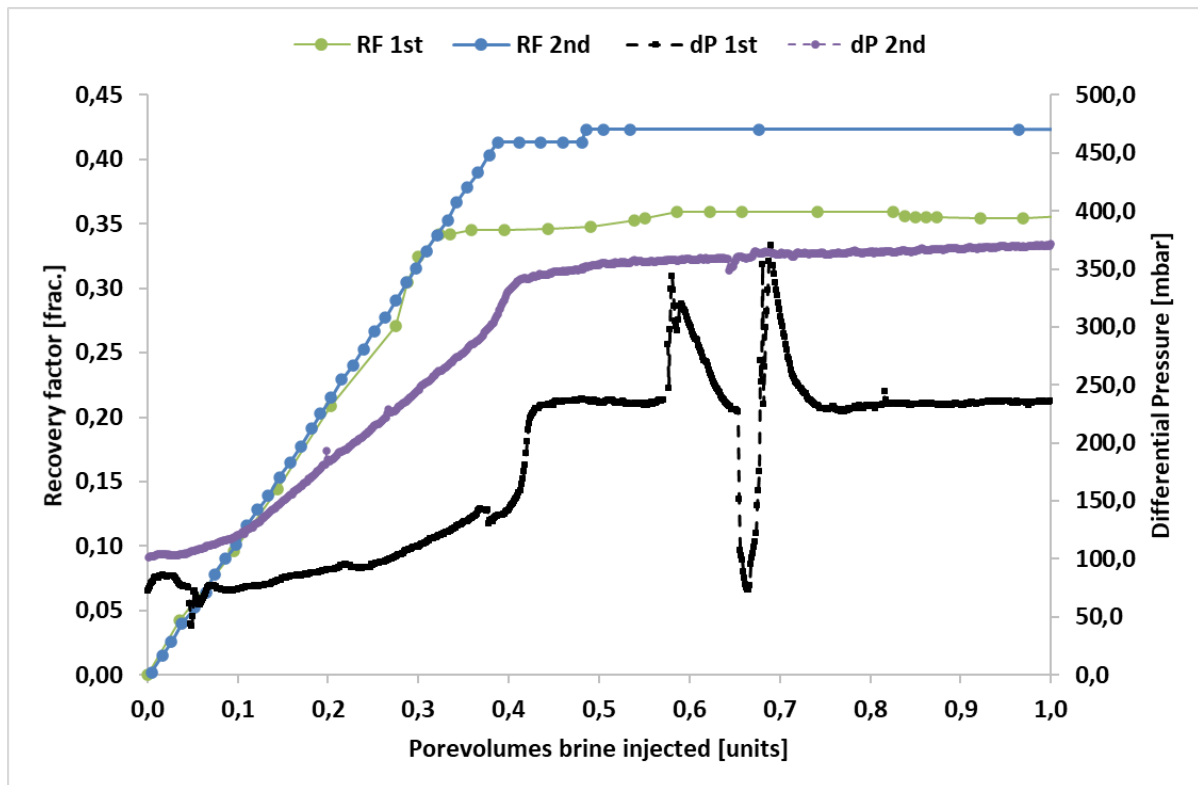


Figure 4-14: Comparison of repeated forced imbibition experiment on core 3A with Marcol 82 using rate 2 mL/h. Pore volumes brine injected is plotted against water saturation and differential pressure.

The effect of injection rate on oil recovery during forced imbibition has been discussed and studied through many years. Some studies have reported that a higher injection rate yields higher recovery, others have reported that the rate does not have a significance to the oil recovery, while others again have observed lower recovery with higher injection rates. (Rapoport & Leas, 1953) For the experiments performed on core 3B, the recovery factor increases when using a lower rate, while $k_w(S_{or})$ decreases. The same trend can be seen in core 3A for the last two experiments. However, looking at the first experiment performed on 3A, for which the rate 2 mL/h was used, it had a lower recovery factor than both experiments performed afterwards. Since it was performed on a different setup which in theory could trap some oil it could perhaps help explain the seeming lower recovery factor, but the lower dP indicate that the recorded recovery factor is true.

A different trend that fit with all five experiments is the drop in relative water permeability and the increase in recovery factor for each consecutive experiment. This would indicate that

the experiments themselves affect the cores and give rise to a change which give different results (see section 4.3.4 for possible causes). In general, there are too few samples and/or too few experiments to be able to give a definitive answer as to which trend is correct, if any. In all the forced imbibition experiments the oil production was linear and piston-like, following the same overlapping line, but some cores continued producing and got higher recovery factors before breakthrough. After breakthrough the production was stable practically immediately except the third experiment on 3A which produced a little bit after another 0.1 pore volume and the initial experiment with burette which produced a bit more after 0.2 pore volumes. After 1 pore volume all recovery factors were completely stable until the experiments were stopped.

It was also observed that even though the oil production had stopped, the differential pressure kept increasing in several experiments without any further oil being produced. See Figure 4-15 for a comparison of the delta pressure for all five forced imbibition experiments. Note that experiment 3A.2nd Marcol 82 15 mL/h is plotted on the secondary vertical axis to avoid its high values from compressing the other data series. Since no more oil production is registered after 1 pore volume the saturation should be stable after that point. A slowly increasing differential pressure which seem to slowly stabilize over time indicate that there is something happening inside the cores. A physical change in the cores as discussed previously is a possibility. A slow redistribution of saturation inside the core would also give rise to a change in dP with the water saturation increasing at the outlet end of the core due to end effects. Based on the limited data available it is not possible to conclude to the cause of this effect.

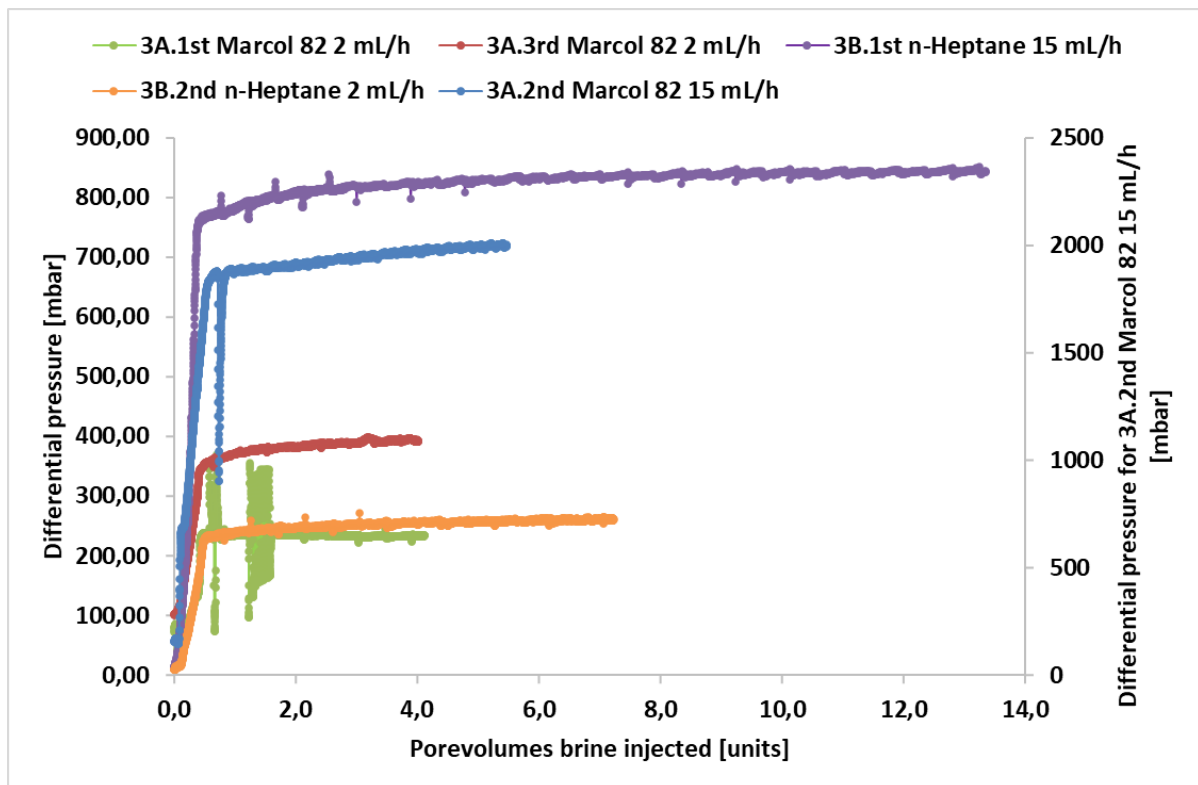


Figure 4-15: Comparison of differential pressure recorded for all five forced imbibition experiments for the full duration of the experiments. Note that the data from experiment 3A.2nd Marcol 82 15 mL/h is plotted on the secondary vertical axis.

5. Conclusion

Six spontaneous imbibition experiments and five forced imbibition experiments were performed in this thesis. Two oils with different viscosities were used, Marcol 82 and n-Heptane. During the forced imbibition experiments two different injection rates were used, 2 mL/h and 15 mL/h.

From the spontaneous imbibition results, one could see that the effect of viscosity ratio did not affect the imbibition rate of very much, because of the low relative water permeability. A big difference in the results of some of the SI experiments could be observed. This could be due to several different things, like for example physical changes in the cores, and it is therefore not possible to conclude without doing more experiments.

For the forced imbibition results a surprising trend of decreasing water permeability and increasing S_{or} could be observed. There could also be said to be a trend where the recovery

factor increases with a lower injection rate. These trends could be coincidences, and there are too few experiments performed in order to conclude anything for sure.

6. Suggestions for Further Work

In order to get more reliable results more experiments should be carried out. It would be interesting to perform the same experiments on different cores to see if the differences in results were due to physical changes in the cores or not.

References

- Abdallah, W., Buckley, J. S., Carnegie, A., Edwards, J., Herold, B., Fordham, E., . . . Signer, C. (1986). Fundamentals of wettability. *Technology*, 38(1125-1144), 268. Retrieved from http://www.ipt.ntnu.no/~kleppe/TPG4150/Oilfield_Review_Fundamentals_of_Wettability.pdf
- Austad, T., & Kolnes, J. Reservoir Engineering - Part II. In *Reservoir Engineering*.
- Civan, F., & Donaldson, E. (1989). Relative permeability from unsteady-state displacements with capillary pressure included. *SPE Formation Evaluation*, 4(02), 189-193. doi:<https://doi.org/10.2118/16200-PA>
- Craig, J. F. F. (1971). *The Reservoir Engineering Aspects of Waterflooding*. Dallas: Society of Petroleum Engineers of AIME.
- Kleppe, J., & Morse, R. A. (1974). *Oil production from fractured reservoirs by water displacement*. Paper presented at the Fall Meeting of the Society of Petroleum Engineers of AIME.
- Leverett, M. C. (1941). Capillary behavior in porous solids. *Transactions of the AIME*, 142(01), 152-169. doi:<https://doi.org/10.2118/941152-G>
- Ma, S., Morrow, N. R., & Zhang, X. (1997). Generalized scaling of spontaneous imbibition data for strongly water-wet systems. *Journal of Petroleum Science and Engineering*, 18(3), 165-178. doi:[https://doi.org/10.1016/S0920-4105\(97\)00020-X](https://doi.org/10.1016/S0920-4105(97)00020-X)
- Mahmood, S. M., & Honarpour, M. (1988). Relative-Permeability Measurements: An Overview. *Journal of Petroleum Technology*, 40(8), 963-966. doi:10.2118/18565-PA
- Mason, G., & Morrow, N. R. (2013). Developments in spontaneous imbibition and possibilities for future work. *Journal of Petroleum Science and Engineering*, 110, Pages 268-293. doi:<https://doi.org/10.1016/j.petrol.2013.08.018>
- Mattax, C. C., & Kyte, J. (1962). Imbibition oil recovery from fractured, water-drive reservoir. *Society of Petroleum Engineers Journal*, 2(02), 177-184. doi:<https://doi.org/10.2118/187-PA>
- Morrow, N. R., & Mason, G. (2001). Recovery of oil by spontaneous imbibition. *Current Opinion in Colloid & Interface Science*, 6(4), 321-337. doi:[https://doi.org/10.1016/S1359-0294\(01\)00100-5](https://doi.org/10.1016/S1359-0294(01)00100-5)
- Odeh, A., & Dotson, B. (1985). A method for reducing the rate effect on oil and water relative permeabilities calculated from dynamic displacement data. *Journal of Petroleum Technology*, 37(11), 2,051-052,058. doi:<https://doi.org/10.2118/14417-PA>
- Rapport, L., & Leas, W. (1953). Properties of linear waterfloods. *Journal of Petroleum Technology*, 5(05), 139-148. doi:<https://doi.org/10.2118/213-G>
- Richardson, J., Kerver, J., Hafford, J., & Osoba, J. (1952). Laboratory determination of relative permeability. *Journal of Petroleum Technology*, 4(08), 187-196. doi:<https://doi.org/10.2118/952187-G>
- Terry, R. E., & Rogers, J. B. (2015). *Applied Petroleum Reservoir Engineering* (Third ed.). United States: Pearson Education, Inc.
- Warner, H. R. H. J. (2015). *The Reservoir Engineering Aspects of Waterflooding* (Second ed.). Richardson, TX 75080-2040 USA: Society of Petroleum Engineers.
- Zhou, D., Jia, L., Kamath, J., & Kovscek, A. (2002). Scaling of counter-current imbibition processes in low-permeability porous media. *Journal of Petroleum Science and*

Engineering, 33(1-3), 61-74. doi:[https://doi.org/10.1016/S0920-4105\(01\)00176-0](https://doi.org/10.1016/S0920-4105(01)00176-0)

Zolotukhin, A. B., & Ursin, J.-R. (2000). *Introduction to petroleum reservoir engineering*: Norwegian Academic Press (HøyskoleForlaget).